Turbulence Measurements During Spring of 1994 at Apache Point Observatory

by Frank D. Eaton, John R. Hines,
and William H. Hatch
Battlefield Environment Directorate

James J. Drexler and James Northrup
Lockheed Engineering and Sciences Company

DTIC
SELECTED
JUL 1 4 1995
G

April 1995

19950711 019

NOTICES

Disclaimers

The findings in this report are not to be construed as an official Department of the Army position, unless so designated by other authorized documents.

The citation of trade names and names of manufacturers in this report is not to be construed as official Government indorsement or approval of commercial products or services referenced herein.

Destruction Notice

When this document is no longer needed, destroy it by any method that will prevent disclosure of its contents or reconstruction of the document.

REPORT DOCUMENTATION PAGE

1. AGENCY USE ONLY *(Leave blank)*	2. REPORT DATE April 1995	3. REPORT TYPE AND DATES COVERED Final 21 May through 25 Jun 94	

4. TITLE AND SUBTITLE

Turbulence Measurements During Spring of 1994
at Apache Point Observatory

5. FUNDING NUMBERS

6. AUTHOR(S)

Frank D. Eaton, John R. Hines, and William H. Hatch (BED)
James J. Drexler and James Northrup (LESC)

7. PERFORMING ORGANIZATION NAME(S) AND ADDRESS(ES)

U.S. Army Research Laboratory
Battlefield Environment Directorate
Attn: AMSRL-BE-E
White Sands Missile Range, NM 88002-5501

8. PERFORMING ORGANIZATION REPORT NUMBER

ARL-TR-560

9. SPONSORING / MONITORING AGENCY NAME(S) AND ADDRESS(ES)

U.S. Army Research Laboratory
2800 Powder Mill Road
Adelphi, MD 20783-1145

10. SPONSORING / MONITORING AGENCY REPORT NUMBER

ARL-TR-560

11. SUPPLEMENTARY NOTES

12a. DISTRIBUTION / AVAILABILITY STATEMENT

Approved for public release; distribution is unlimited.

12b. DISTRIBUTION CODE

13. ABSTRACT *(Maximum 200 words)*

Optical turbulence measurements taken using the Atmospheric Turbulence Measurement and Observation System (ATMOS) and an acoustic sounder at the newly established Apache Point Observatory (APO) are presented for spring 1994. APO is located at 9200 ft MSL about 18 mi south of Cloudcroft, NM. The ATMOS is an optical device for determining seeing conditions by measuring angle-of-arrival fluctuations through two subapertures of a telescope. This optical arrangement, utilizing a differential measurement technique, eliminates errors caused by tracking, vibration, and wind loading.

Results include all r_0 measurements, the surface wind measured at nearby Sacramento Peak, time-height displays of sodar observations, and wind and C_n^2 profile measurements taken with a 50-MHz radar located in the Tularosa Basin. A method under development to predict optical turbulence at APO is briefly discussed.

14. SUBJECT TERMS

turbulence, r_0, C_n^2, sodar, ATMOS

15. NUMBER OF PAGES

72

16. PRICE CODE

17. SECURITY CLASSIFICATION OF REPORT	18. SECURITY CLASSIFICATION OF THIS PAGE	19. SECURITY CLASSIFICATION OF ABSTRACT	20. LIMITATION OF ABSTRACT
Unclassified	Unclassified	Unclassified	SAR

Contents

Figures

1

3

1. Introduction

The refractive index structure parameter (C_n^2) and derived parameters such as the transverse coherence length (r_o) and the isoplanatic angle (θ_o) are of fundamental importance in understanding optical, radio, and acoustic propagation in the atmosphere and are of considerable interest to many remote sensing efforts. Optical turbulence has imposed a major problem upon optical astronomy, degrading imagery observed with the large telescopes at major observatories. Ground-based optical systems, thermosondes, and remote sensors are used for sensing optical turbulence parameters. [1] High resolution C_n^2 profiles can be obtained from radar or sodar measurements.

Brant et al. [2] provided measured seeing values at several observatories as well as daytime seeing statistics at Sacramento Peak Observatory (SPO), NM. They cautioned comparing absolute values because of different techniques used; different local effects, such as dome seeing; calibration of different systems; and the validity of the particular zenith angle correction used. The measured results from SPO were taken using the solar vacuum telescope with the entrance aperture 40 m above the ground. [2] The r_o values are predicted to exceed those that would be taken using a conventional near-surface dome, because no dome was used and the configuration avoided a large contribution of turbulence from near-ground convection.

The results presented here include r_o values and C_n^2 time-height displays taken at Apache Point Observatory (APO), surface wind measurements taken from nearby SPO, and profiles of C_n^2 and wind measured using a 50-MHz radar at White Sands Missile Range (WSMR), NM.

2. Site

APO is an astronomical observatory located in the Lincoln National Forest in the Sacramento Mountains at an altitude of 2800 m (9200 ft) MSL. It is owned and operated by the Astrophysical Research Consortium consisting of the University of Chicago, Institute of Advanced Study, Johns Hopkins University, New Mexico State University, Princeton University, University of Washington, and Washington State University. APO was recently established for operation (10 May 94) when the 3.5-m multipurpose telescope observed a solar eclipse. This telescope is located at 32° 46' 50.4" N, 105° 49' 11.7" W. Three other telescopes at APO are in various stages of completion.

One unique-purpose telescope under design is the Sloan Digital Sky Survey (SDSS) telescope that will be used under appropriate seeing conditions to survey the night sky with sensitive imaging equipment. The enclosure for the SDSS telescope was constructed on pillars west of the mountain ridge to reduce degrading turbulent conditions, because excellent seeing is a requirement for this effort. The Atmospheric Turbulence Measurement and Observation System (ATMOS) used in this study was mounted atop the pedestal constructed for future installation of the 2.5-m SDSS telescope. The sodar was installed on the ridge southeast of the SDSS enclosure.

The 50-MHz radar used in this study is located at 32° 24' N, 106° 21' W at 1220 m MSL; approximately 13 km east of the post area at WSMR, NM. It is one of four radar systems operated at the Atmospheric Profiler Research Facility (APRF) in the Tularosa Basin about 25 km east of the Organ Mountains and 68 km southeast of APO. The local area of the APRF is characterized by flat terrain covered with low brush. The APRF is upwind of APO because the prevalent winds in the area are generally southwesterly to westerly.

3. Methodology

Measurements were taken at APO on 21, 22, and 23 May and 8, 9, 23, 24, and 25 Jun 94 to examine the turbulent conditions during late spring at the SDSS site. The tests involved the use of two systems at APO: ATMOS and a single-axis sodar. Simultaneous profile measurements of wind and C_n^2 were taken using the 50-MHz radar at the APRF. Supporting surface measurements of wind were taken using a Surface Atmospheric Measurement System (SAMS) at the National Solar Observatory at Sacramento Peak.

3.1 ATMOS

The classical astronomical seeing problem was put on a more quantitative basis than in the past by the formulation of the transverse coherence length (r_o): [3]

$$r_o = [0.423k^2 \int_o^\infty C_n^2(z)dz]^{-3/5} \tag{1}$$

where

$$
\begin{aligned}
k &= 2\pi/\lambda \ (\lambda \text{ is the wavelength of light}) \\
C_n^2 &= \text{refractive index structure parameter} \\
z &= \text{altitude above ground for vertical viewing.}
\end{aligned}
$$

Effects of atmospheric turbulence on optical systems sensitive to wavefront distortions can be conveniently evaluated with knowledge of r_o. Selection and evaluation of observatory sites traditionally required an examination of astronomical seeing. Methods to appraise seeing have been used for over 50 yr, including measurements of image spread and motion by photographing star trails and photoelectric detection of scintillation. [4,5,6,7] The Polaris seeing monitor was used for the site selection of Kitt Peak National Observatory. [8] The literature displays a natural application of the evolution of technology to seeing monitors, such as replacing film techniques with linear-array charge-coupled devices (CCDs) and, finally, CCD cameras. The analyses of line-spread function information, obtained from stellar images using linear-array CCDs to

obtain r_o from the modulation transfer function as well as the differential image motion technique used in this study, are documented by Eaton et al. [9] Roddier [10] and Fried [11] summarized the single and differential image motion techniques for evaluating seeing conditions.

ATMOS uses a differential angle-of-arrival approach by collecting light from a single star with two subapertures (11-cm diameter) on a 35.5-cm (14-in.) diameter telescope. The subapertures have optical glass wedges so the two images can be separated and focused onto a two-dimensional CCD camera placed at the focal plane. Two nearly parallel paths of turbulence are measured at 23.5 cm separation. The method eliminates common system errors caused by tracking errors, vibration, and wind loading, because such effects will display identical image motion and not be included in the variance of centroid differences. ATMOS includes a frame grabber that can vary exposure time and frame rates to more than 300 frames/s. The CCD camera is intensified and uses an electronic shutter capable of exposure times as short as 20 μs.

The relationship used in this study to calculate r_o with ATMOS is

$$r_o = \{\frac{27.5\ F^2}{k^2\ d^{1/3}\sigma_r^2}[1-\frac{25}{36}(\frac{d}{\mu})^{1/3}]\}^{3/5} \tag{2}$$

where

F	=	the focal length of the receiving telescope
d	=	the diameter of each subaperture
μ	=	center-to-center separation of the subapertures
σ_r^2	=	mean-square of the relative distance between the centroids of the two images.

3.2 Sodar

Sodar (sonic detection and ranging) detects the temperature structure function (C_T^2) and, ultimately, provides C_n^2 through calculations using simultaneously sampled ambient temperature and pressure values.

The sodar equation is

$$C_T^2 = \frac{P_r T_o^2 e^{2\bar{\alpha}R} L_e}{E_r [P_t \cdot E_t][(\frac{c\tau}{2})(\frac{A}{R^2} \cdot G)][0.0039 k^{1/3}]}$$

(3)

where

P_t	=	transmitted power
P_r	=	received power
R	=	range
k	=	acoustic wave number
T_o	=	surface temperature
α	=	molecular and classical adsorption
E_r	=	receiver efficiency
E_t	=	transmitter efficiency
c	=	speed of sound
τ	=	pulse length
A	=	antenna area
G	=	antenna directivity
L_e	=	excess attenuation coefficient.

The sodar is an Echosonde model single-axis system manufactured by Radian Corporation. Three-axis systems are used for obtaining doppler winds. The sodar is typically operated at 1850 Hz and 75-W transmitted power using a

40-ms pulse length and a 1.5-m (5-ft) diameter antenna. Backscatter is averaged every 10 s in 200 range gates to obtain C_n^2 from 30 to 1024 m AGL. Some researchers obtain C_n^2 values from sodar by comparing the backscattered values to in situ values obtained from tower sensors. Calibration of the sodar used in this study was accomplished by a first principles approach.

3.3 50-MHz Radar

Radar parameters of the 50-MHz radar, operated at a nominal central frequency of 49.25 MHz and located at the APRF at WSMR, are described in Nastrom and Eaton. [12] The system is identical to the NASA 50-MHz radar located at Cape Kennedy, except the WSMR system is calibrated for C_n^2. The NASA system is used for wind shear measurements during space shuttle operations. Received power for the WSMR system is observed for 1 min along each of the three beams to derive C_n^2, wind, and spectral width. Pulse coding applied to each 8-μs transmitted pulse produces 1-μs nominal pulse lengths to provide 150-m resolution along each axis. Sampling is from 3.22 to 20 km MSL altitude in 112 range gates. The performance of this radar is high because of the large antenna (150-m diameter) and 250-kW transmitted peak power, producing a power aperture product of 1 x 10^8 Wm. Nastrom and Eaton [12] showed that upward-propagating gravity waves enhance C_n^2 and mechanical turbulence into the lower stratosphere over WSMR.

4. Results

4.1 Transverse Coherence Length (r_o) Measurements

Transverse coherence length (r_o) measurements were taken during three periods: 21, 22, and 23 May 94; 8 and 9 Jun 94; and 23, 24, and 25 June 94. All results are evaluated for a 0.5-μm wavelength and corrected for zenith viewing. Figures 1, 2, and 3 display the results from the first data set in May. The transverse coherence length r_o is labelled "r-naught" in the figures. Arcturus was sensed during the first 2 h at fairly high zenith angles in a direction over the Tularosa Basin, possibly contributing to the rapid increase in values. Vega was sensed from about 3:00 to 5:00 MST in a direction over forested terrain. The next 2 days of data collection showed values fluctuating from a low near 1 cm to a high around 15 cm with the majority of the values near 8 cm. The next data run, 8 to 9 Jun, showed somewhat higher values on the average, as seen in figures 4 and 5. Figures 6, 7, and 8 present the results for the last data session, 23, 24, and 25 Jun. The values were, in general, low on 23 Jun with a slight trend of increasing r_o values into the first few hours of 24 Jun. Measurements commenced during midafternoon and showed low r_o values, as was expected because of surface convective activity. From about 17:00 to 19:00 MST, r_o increased dramatically from about 2.5 to over 16 cm. This effect is attributed to entering the evening neutral event and is probably enhanced because of the strong solar heating on the west-facing slope above which the measurements were taken. For the remainder of the night, the r_o values fluctuated between about 10 to 14 cm.

Figure 9 shows all the data collected during the 8 days plotted together versus time, which displays the large variability that can be found even for a limited time period and conditions. The least variability shown is during the afternoon hours in which surface turbulence contributes heavily to the total profile. Figure 10 displays a histogram of the total 1368 r_o measurements. Generally, r_o and C_n^2 are found to show a lognormal or near lognormal distribution. [13,14] The distribution (figure 10) would appear more lognormal if there were an even distribution of measurements diurnally, with more low daytime values.

Apache Point Observatory, 21 May 1994
Differential Image Motion r-naught

Figure 1. Transverse coherence length measurements on 21 May 94.

Apache Point Observatory, 22 May 1994
Differential Image Motion r-naught

Figure 2. Transverse coherence length measurements on 22 May 94.

Apache Point Observatory, 23 May 1994
Differential Image Motion r-naught
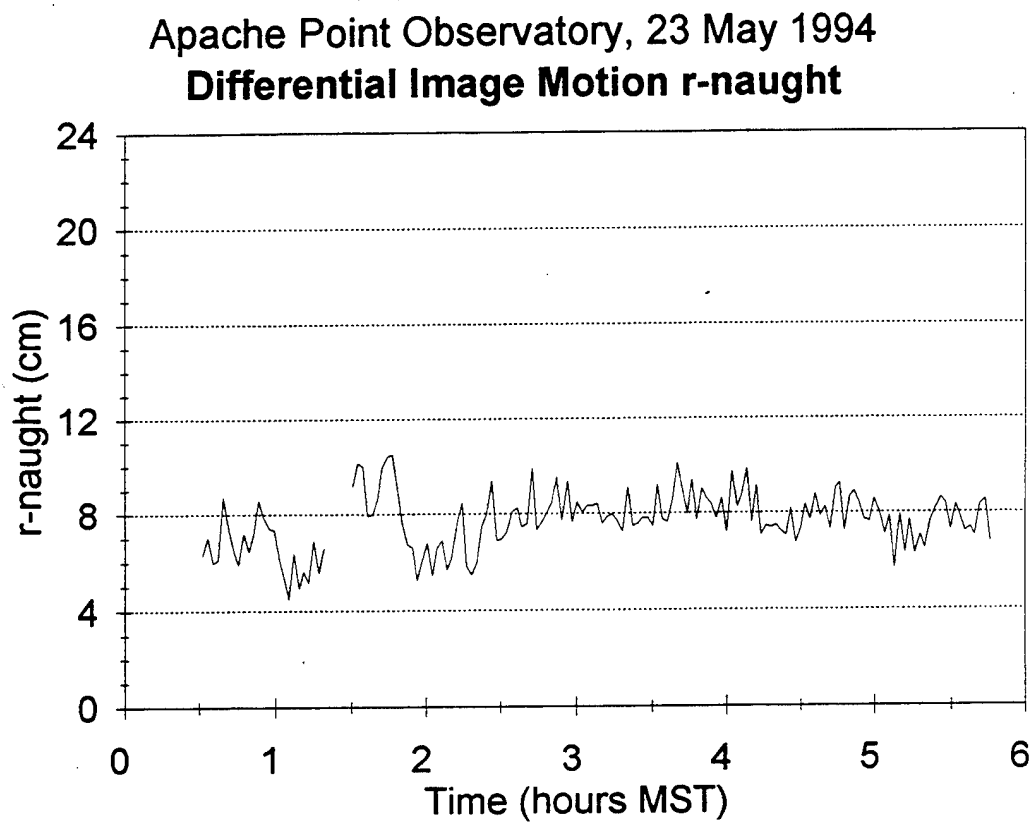
Figure 3. Transverse coherence length measurements on 23 May 94.

Apache Point Observatory, 08 June 1994
Differential Image Motion r-naught
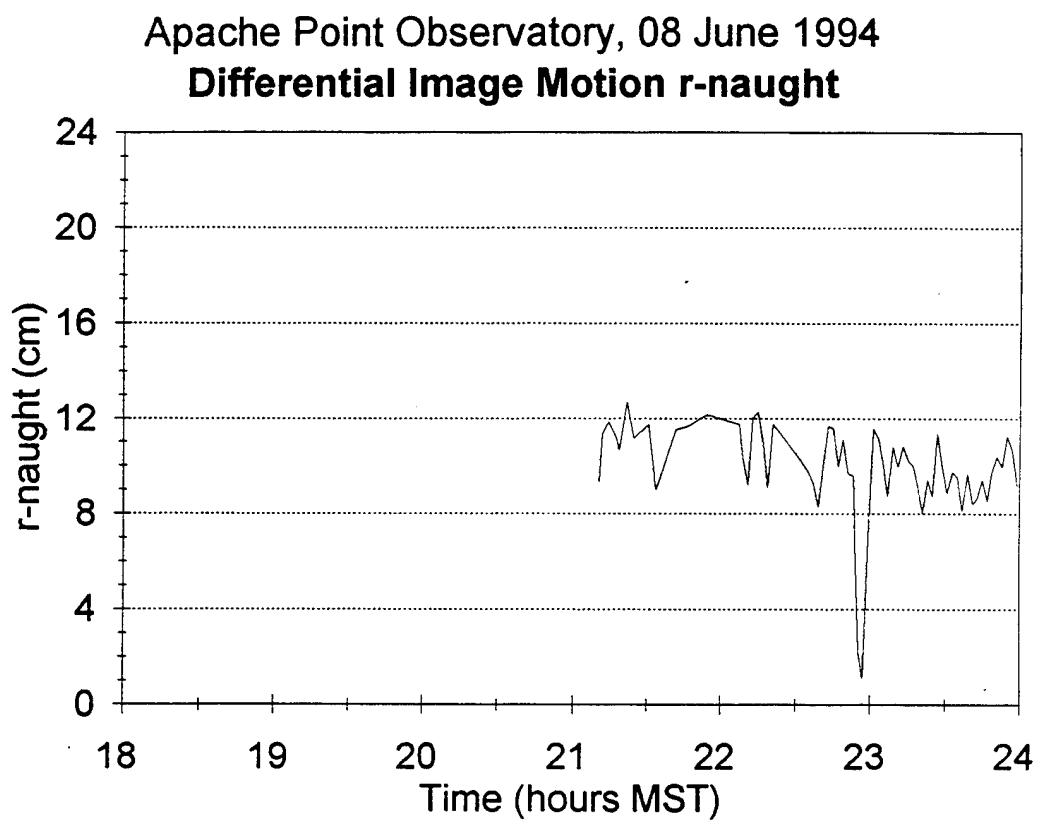
Figure 4. Transverse coherence length measurements on 8 Jun 94.

Apache Point Observatory, 09 June 1994
Differential Image Motion r-naught
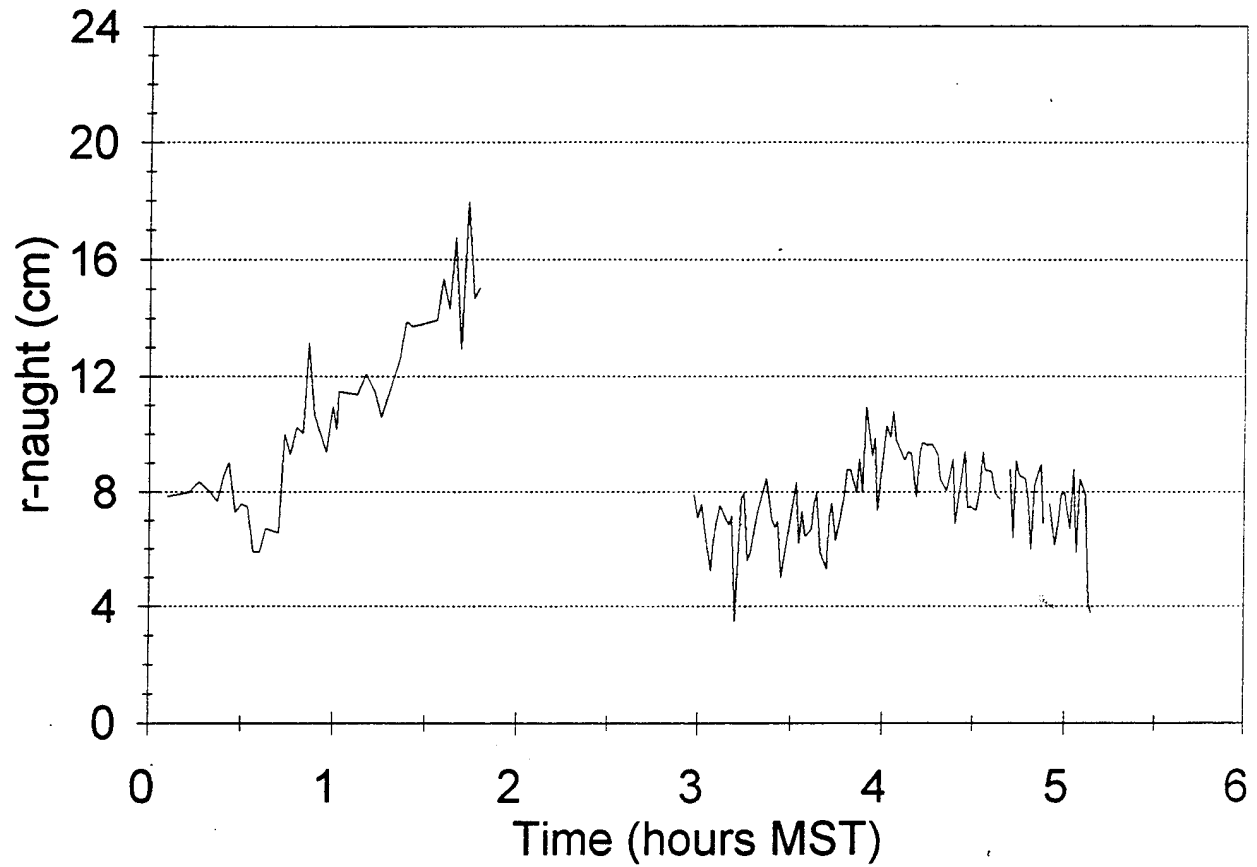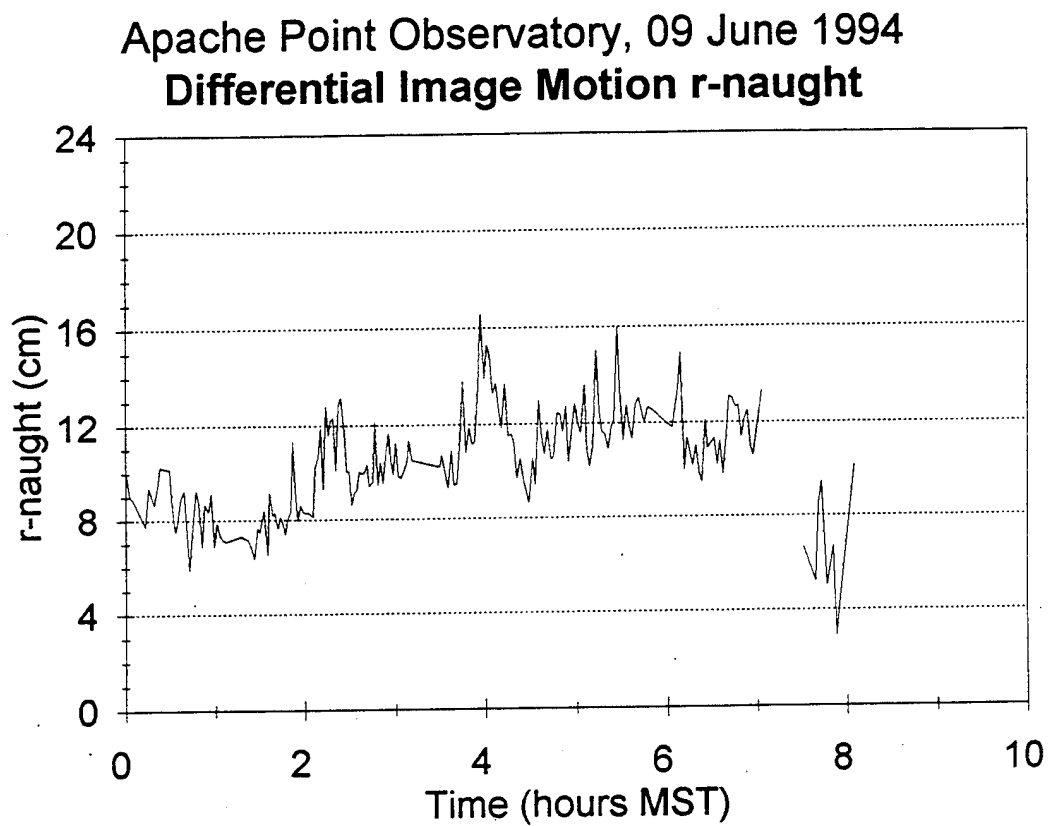

Figure 5. Transverse coherence length measurements on 9 Jun 94.
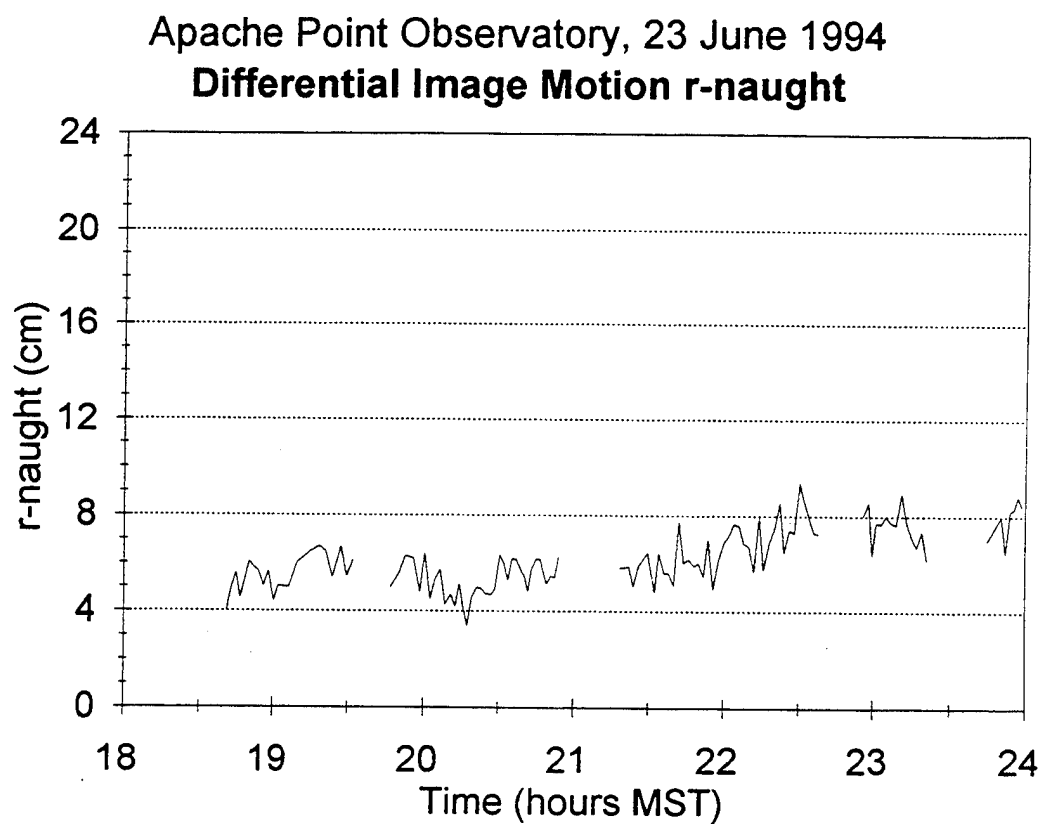
Figure 6. Transverse coherence length measurements on 23 Jun 94.

Apache Point Observatory, 24 June 1994
Differential Image Motion r-naught

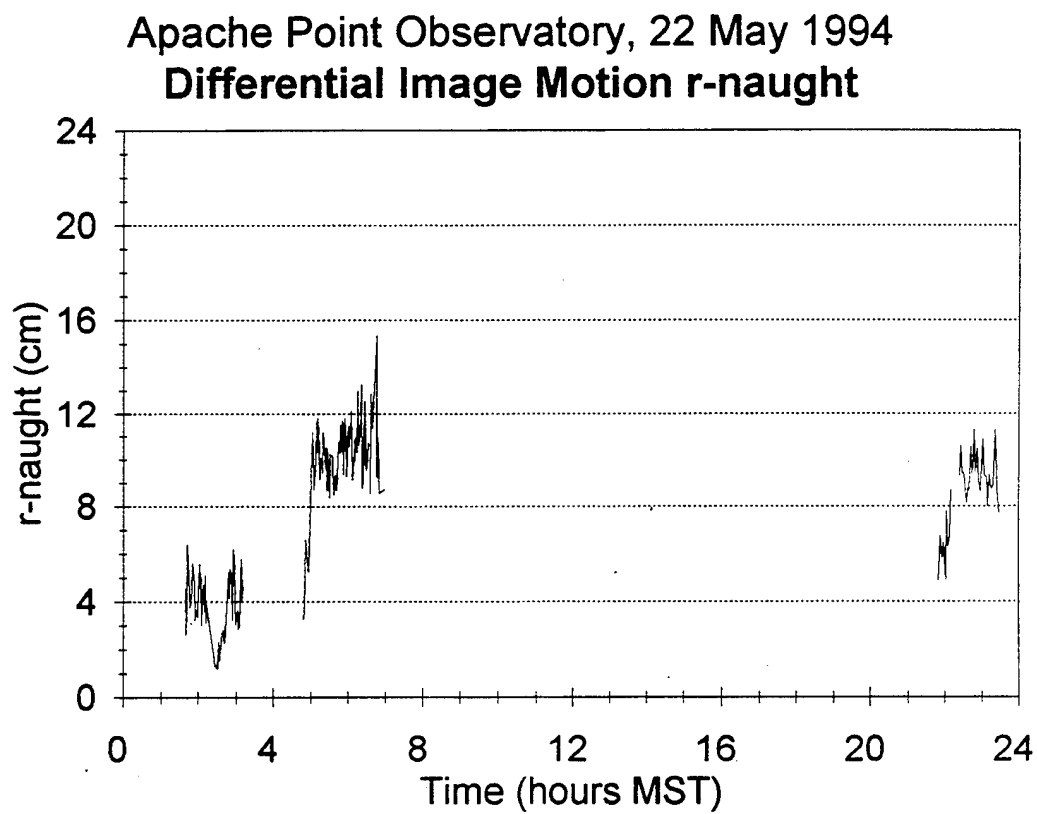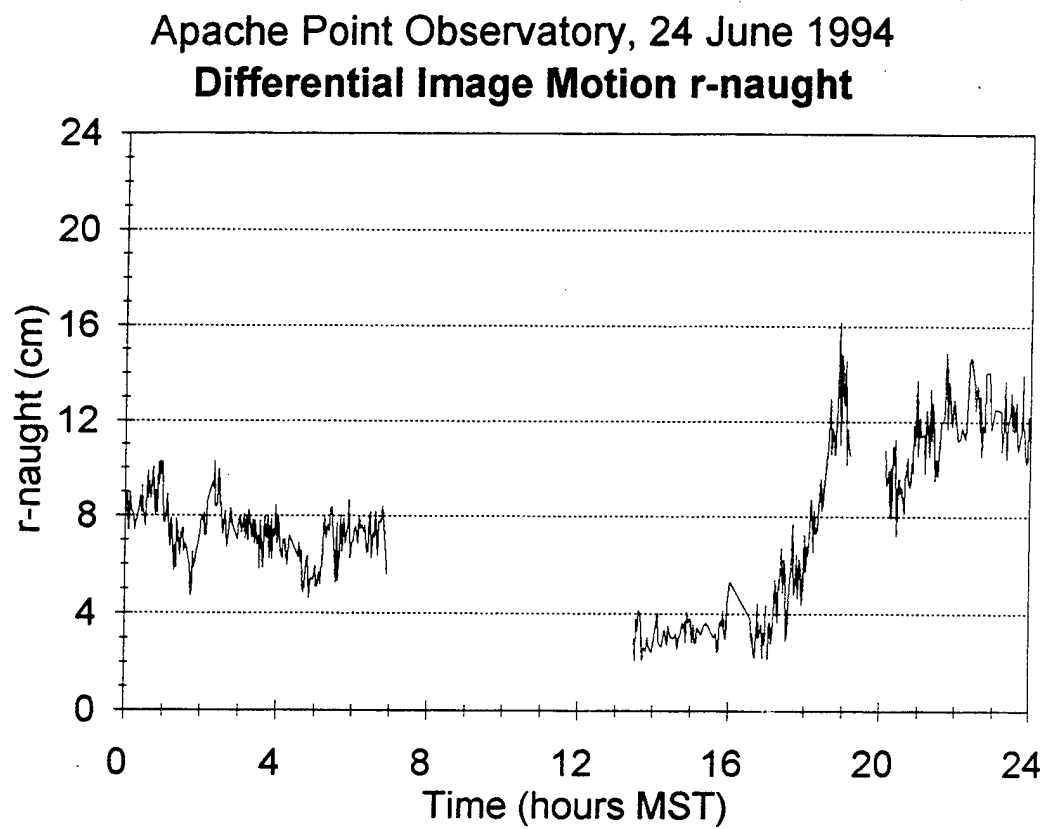**Figure 7. Transverse coherence length measurements on 24 Jun 94.**

Apache Point Observatory, 25 June 1994
Differential Image Motion r-naught
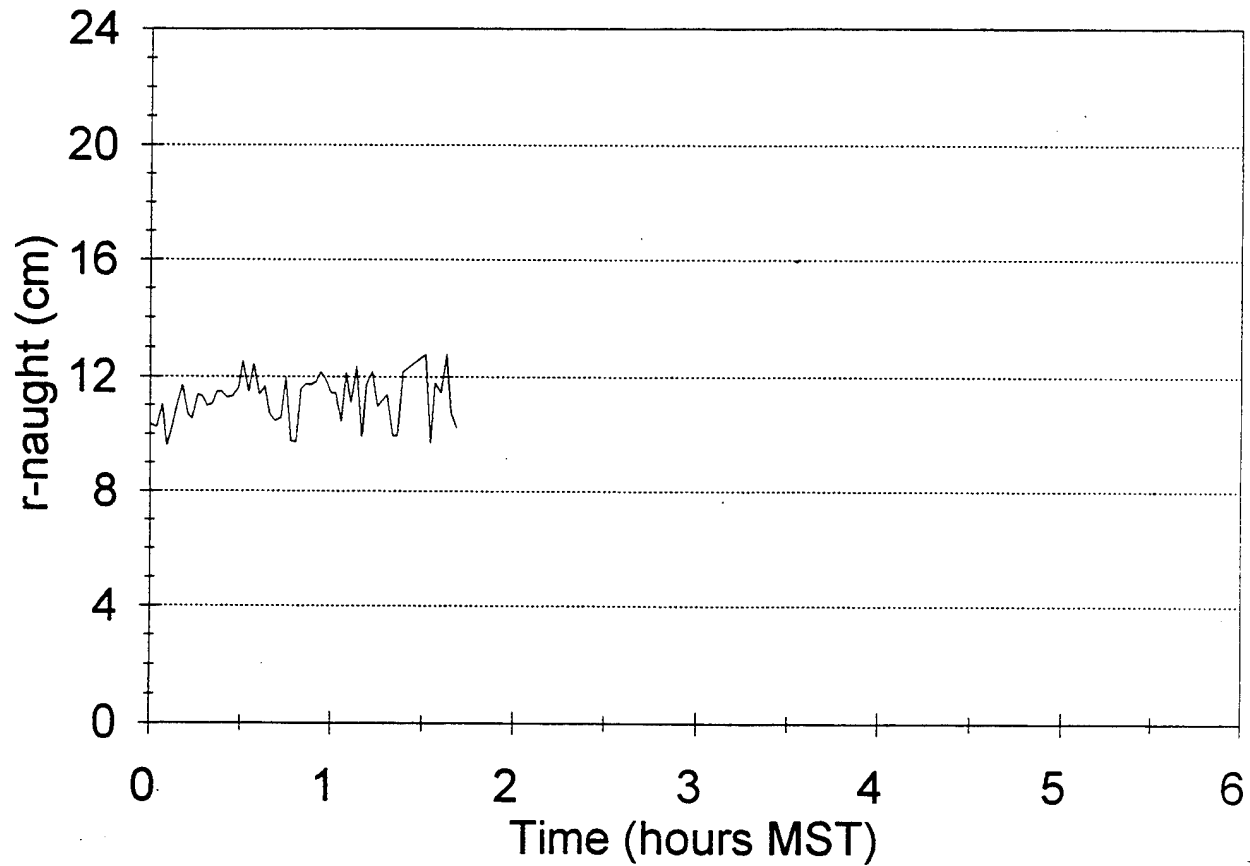
Figure 8. Transverse coherence length measurements on 25 Jun 94.

APO, May and June 1994 Composite
Differential Image Motion r-naught

Legend: • 141 ▪ 142 ▪ 143 ▫ 159 • 160 ◦ 174 ▾ 175 ▴ 176
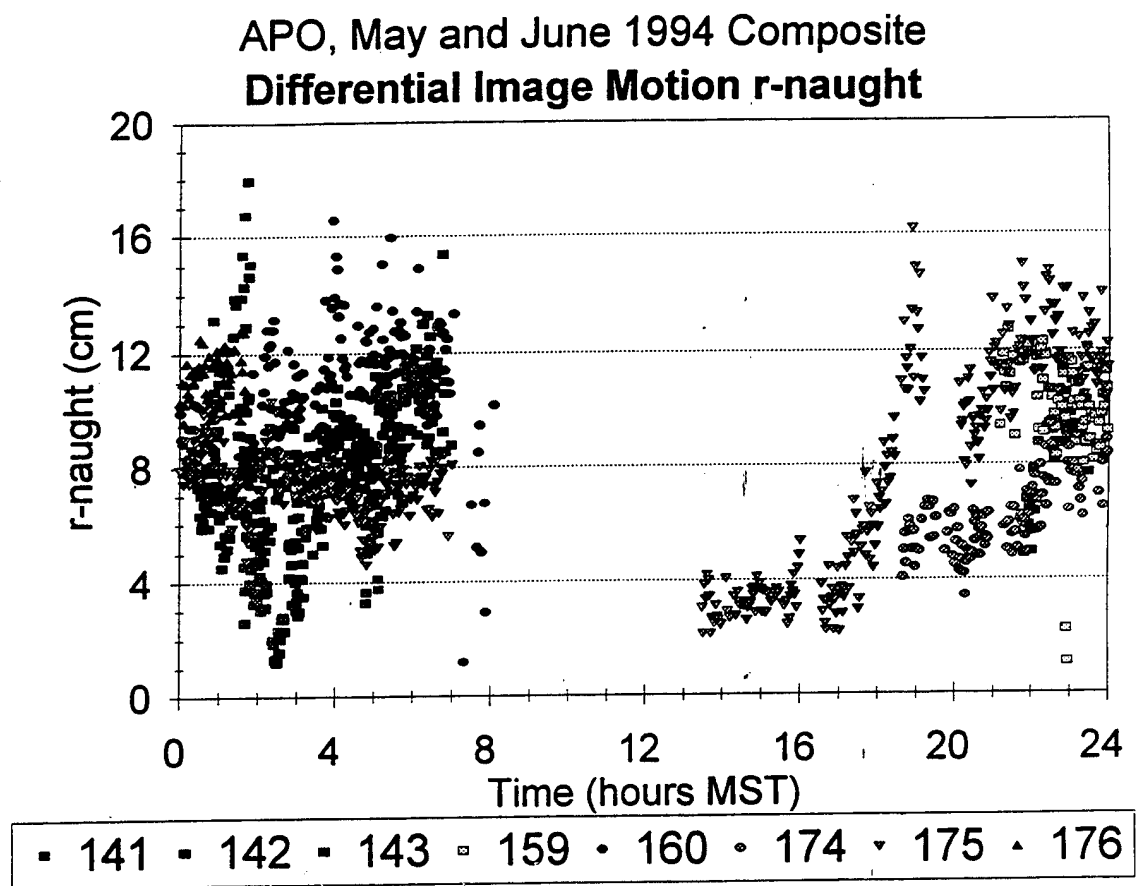
Figure 9. Diurnal composite of all data in figures 1 through 8.

Figure 10. Histogram of all r_0 measurements during spring 94.

4.2 Surface Wind Data

The surface wind speed and direction data versus time for the three measurement periods are shown in figures 11, 13, and 15 while figures 12, 14, and 16 show wind roses of direction for the same periods. In general, wind speeds were low, rarely exceeding 5 kn. The wind dir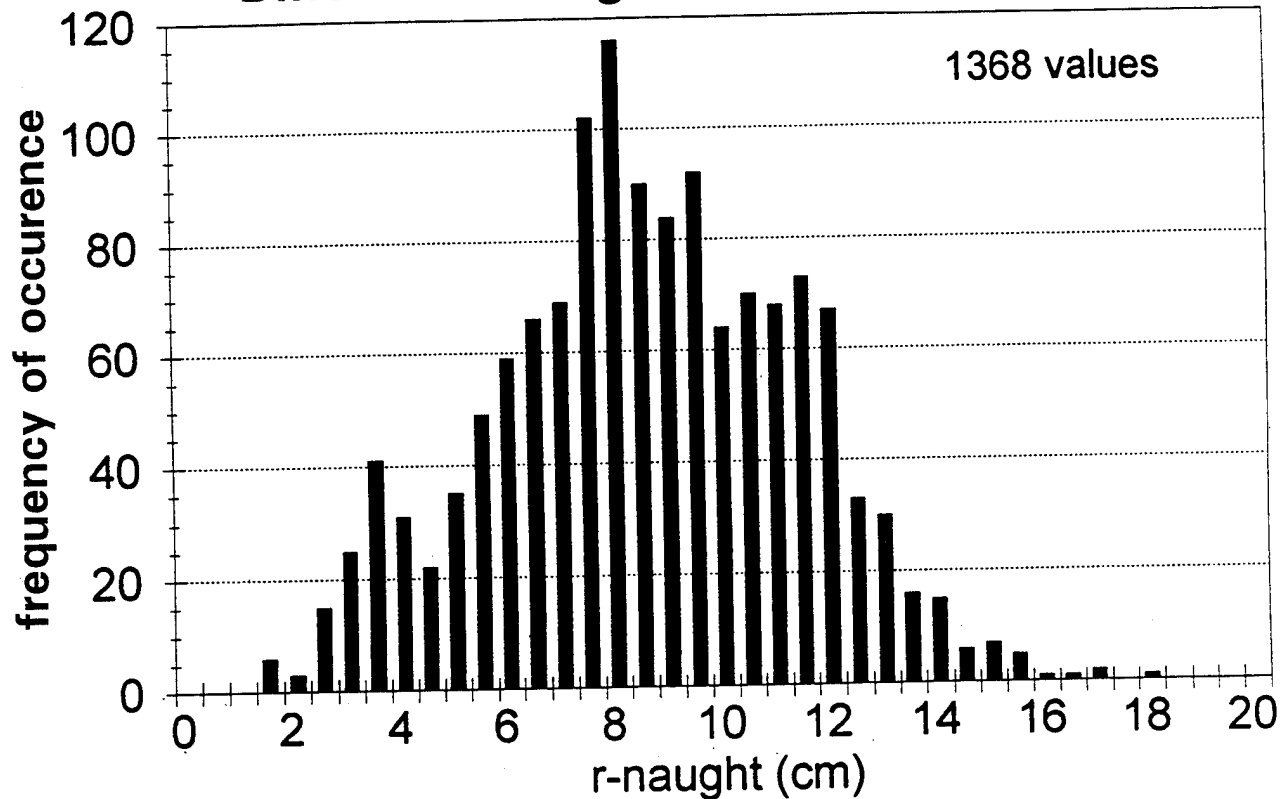ection is of particular interest. It is assumed that well-developed flow from the western side of the ridge will produce the best seeing because of less turbulence being advected from above the Tularosa Basin than from over ground surfaces. There are few examples of flow from the basin direction during the measurement periods. Figure 14 displays a westerly contribution, but figure 13 shows that this is based on a limited number of data points. The westerly flow in figure 16 is mostly during afternoon, a slope-wind effect caused by surface heating.

4.3 Sodar Measurements

Figures 17 through 19 show sodar-obtained time-height displays of backscattered power during times similar to when r_o was measured during the first measurement period. Some wave activity, reaching several hundred meters above the surface, occurs on all 3 days. The sodar results for 9 Jun 94 (figure 20) show the measurements that correspond to the second measurement period. Turbulence was only detected in the lowest part of the profile. The lack of turbulence above this level agrees with the increase of r_o values when compared to the first data session. The last data run (figures 21 through 23) shows a general decrease in nighttime turbulence over the period with considerable wave activity at the beginning. This also agrees with the r_o pattern. Figure 24 is an example of multilayered turbulence at APO, showing the undulations caused by gravity waves. Figure 25 shows an example of a morning transition event with convective activity occurring from about 1500 UTC.
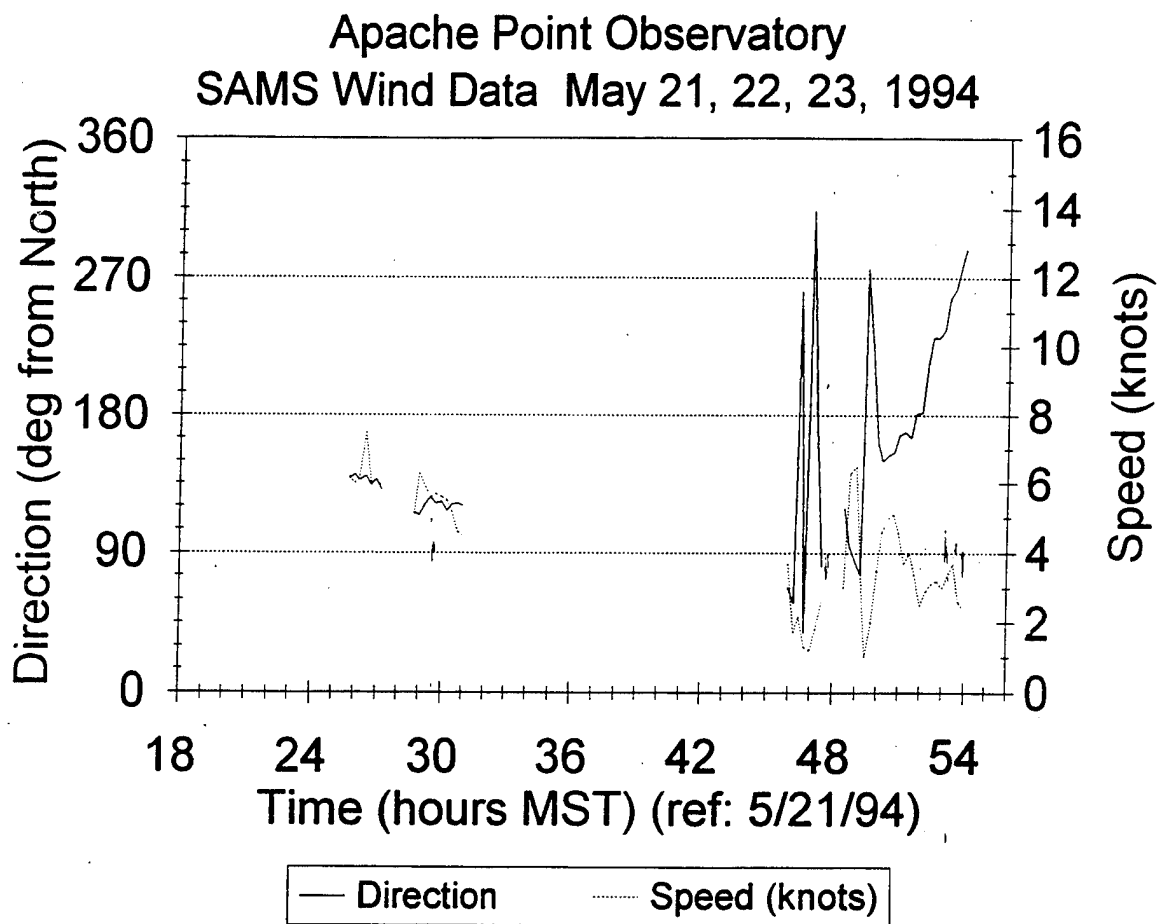
Figure 11. Time series of wind speed and direction for 21, 22, and 23 May 94.

Apache Point Observatory May 21, 22, 23 1994
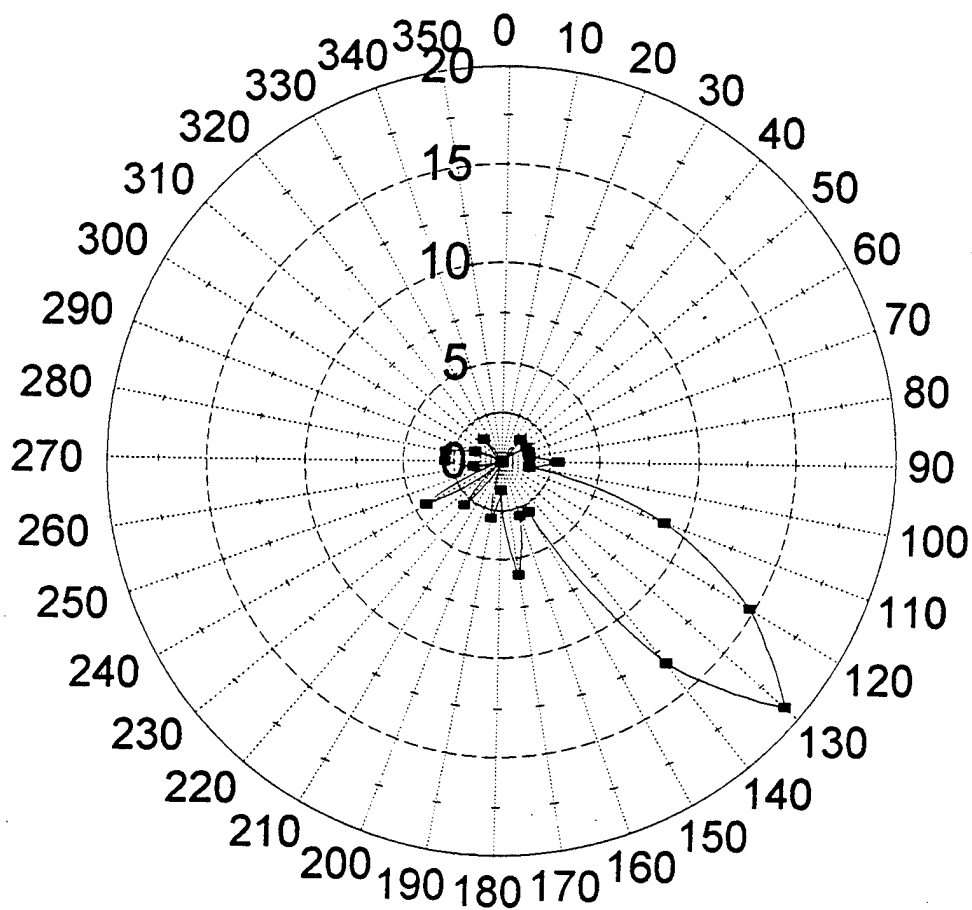
Relative Wind Direction (% of 68 observations)

Figure 12. Wind rose of wind direction for 21, 22, and 23 May 94.
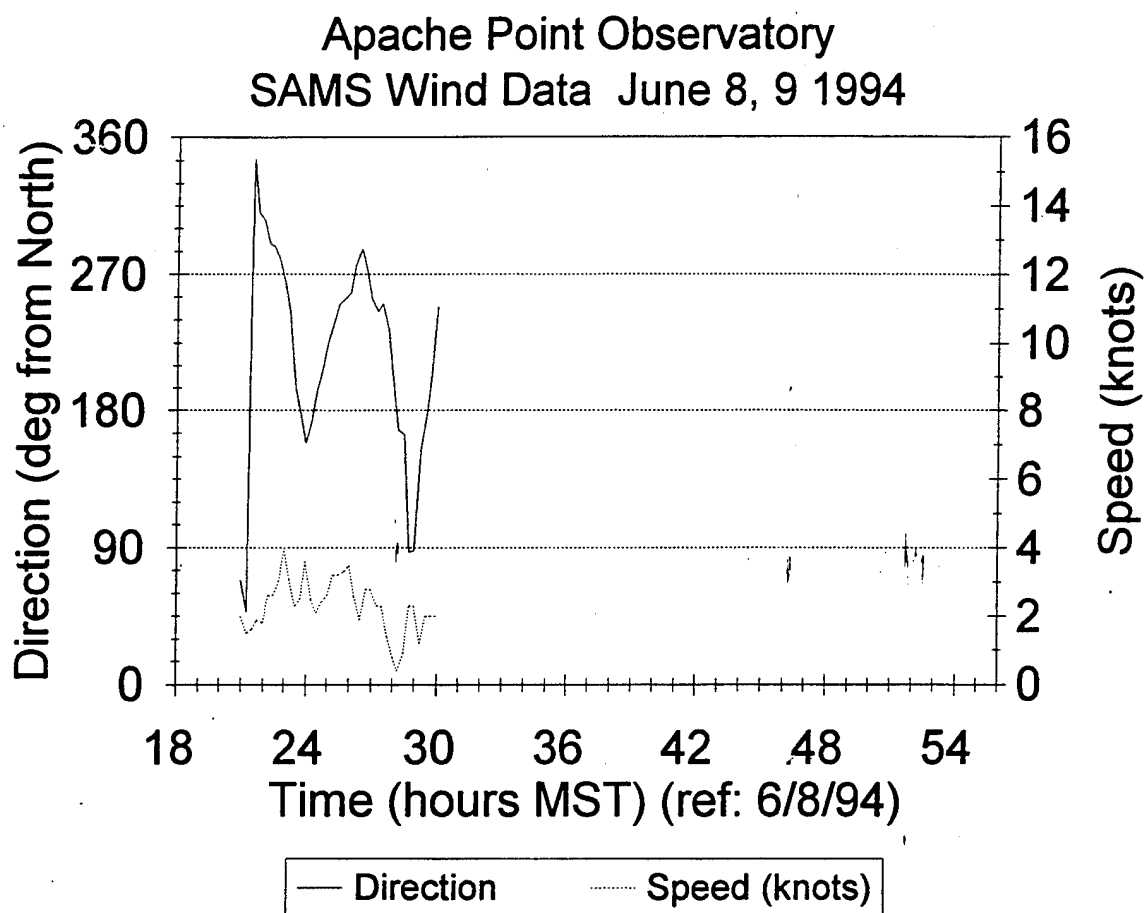
Figure 13. Time series of wind speed and direction for 8 and 9 Jun 94.

Apache Point Observatory June 8 and 9, 1994
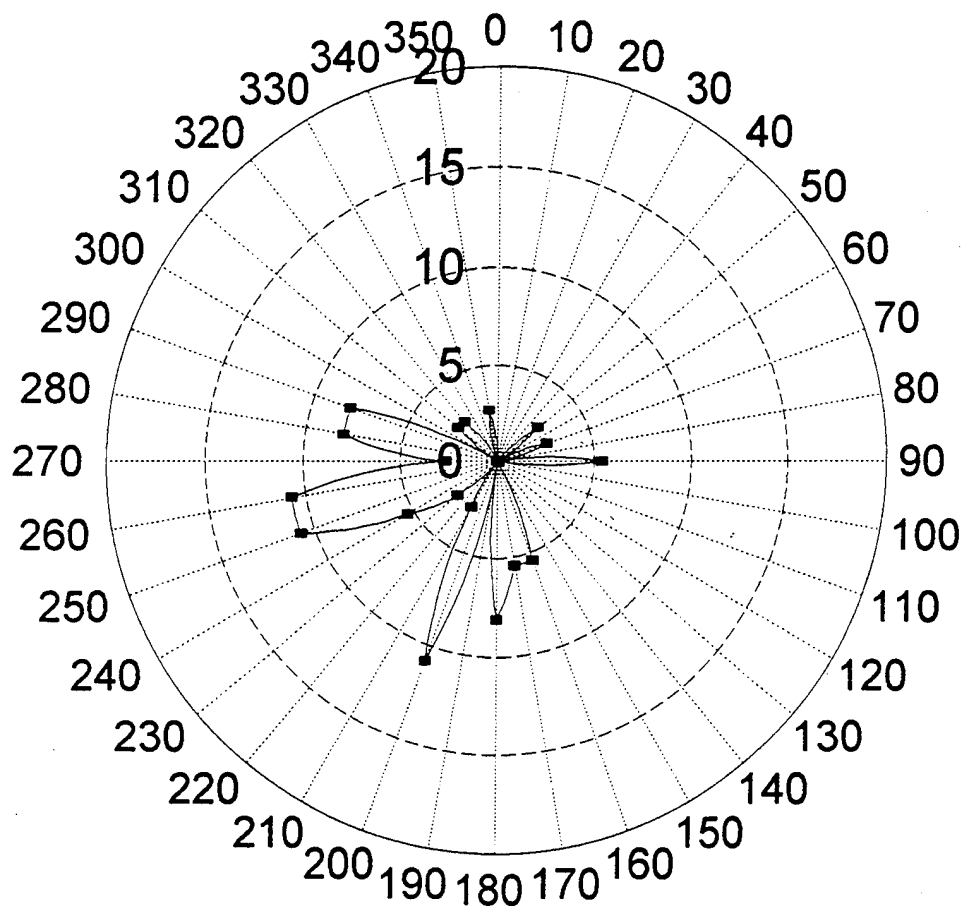
Relative Wind Direction (% of 37 observations)

Figure 14. Wind rose of wind direction for 8 and 9 Jun 94.
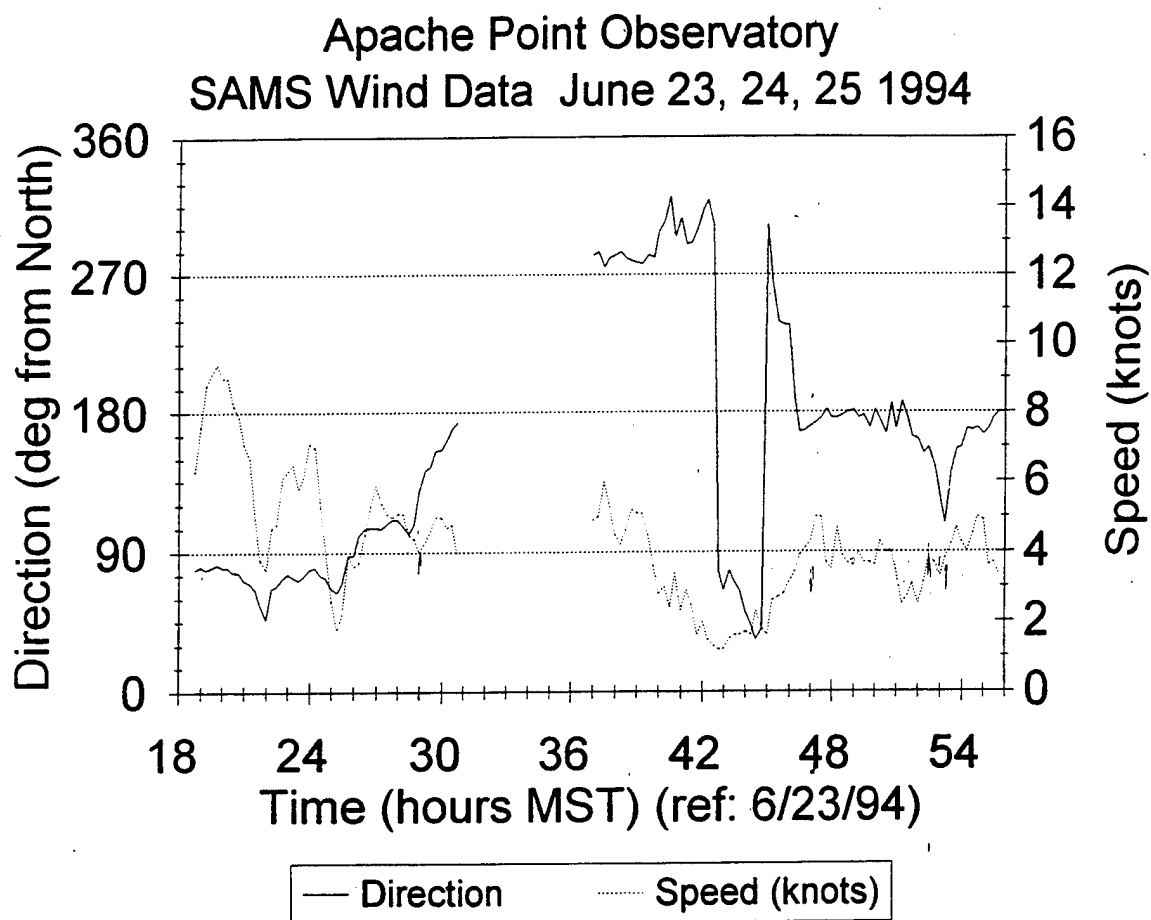
Figure 15. Time series of wind speed and direction for 23, 24, and 25 Jun 94.

Apache Point Observatory June 23,24,25, 1994
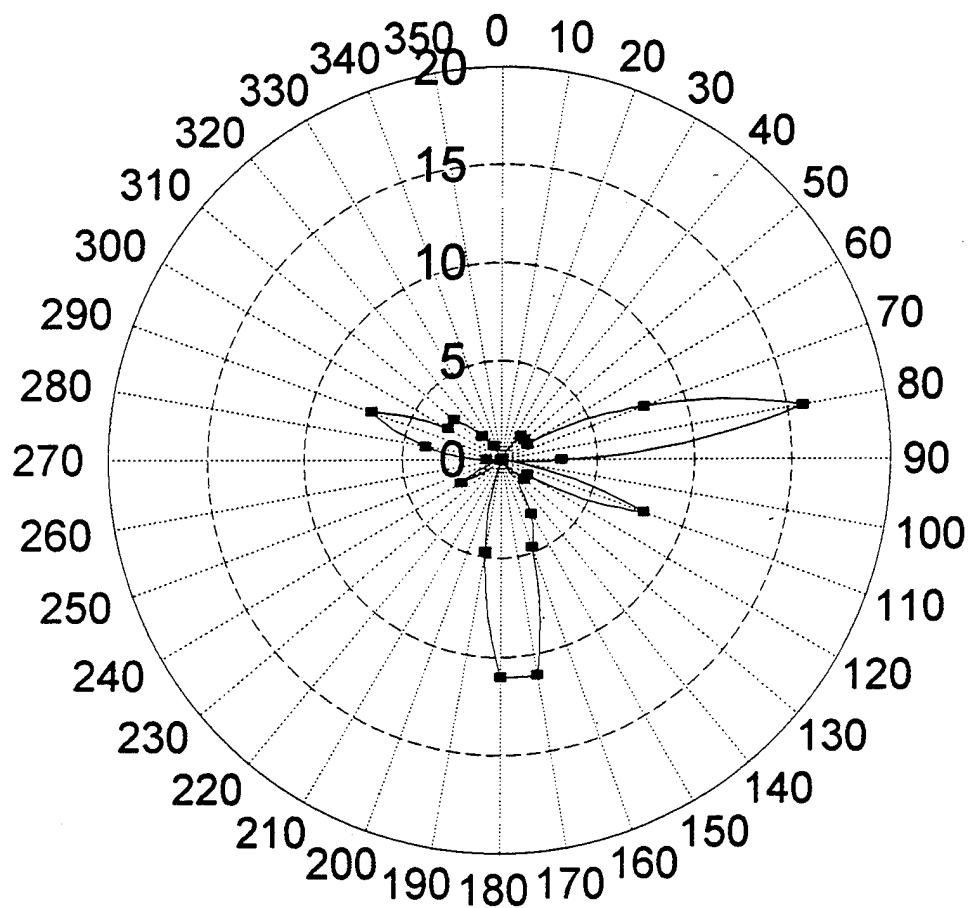
Relative Wind Direction (% of 127 observations)

Figure 16. Wind rose of wind direction for 23, 24, and 25 Jun 94.
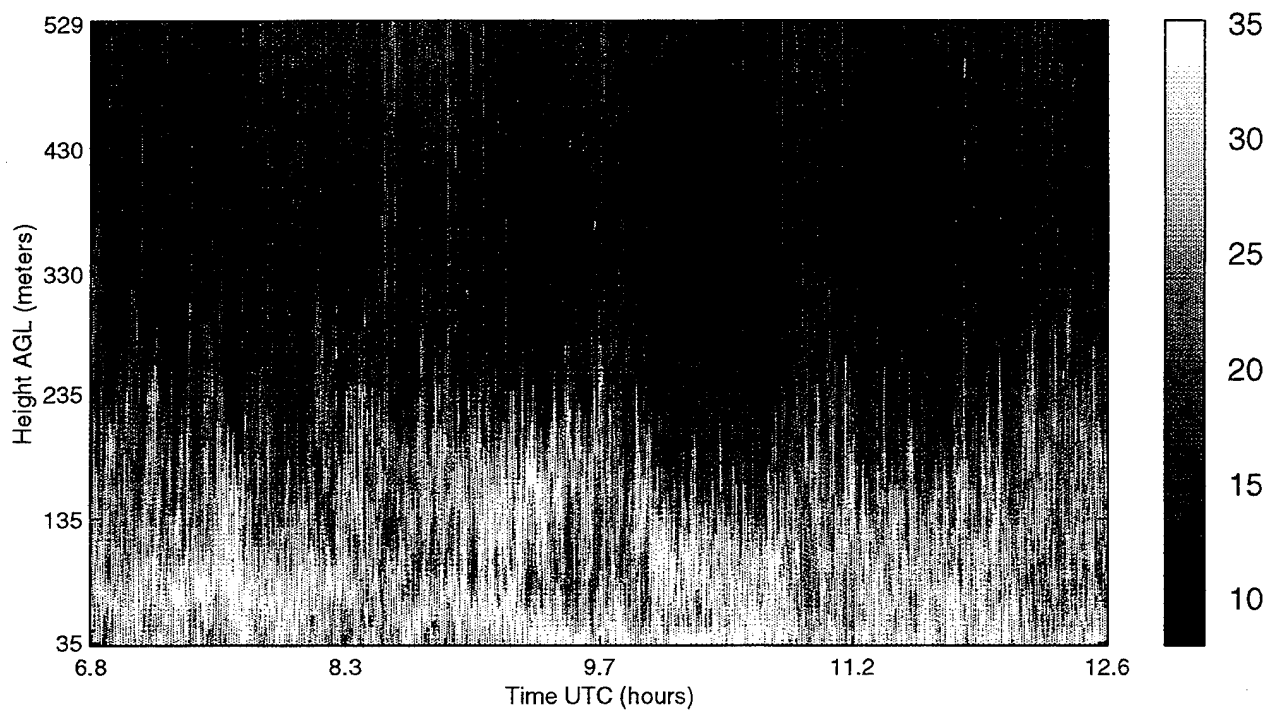
Figure 17. Time-height display of sodar-obtained backscatter on 21 May 94.
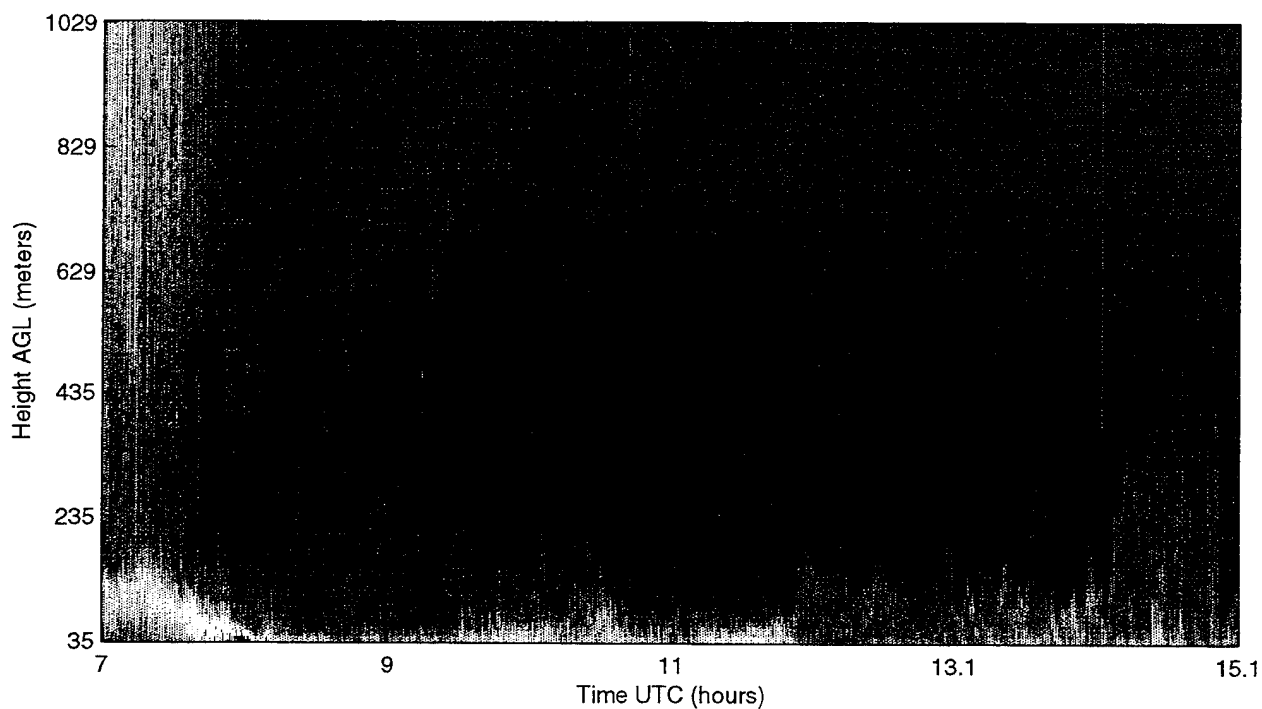
Figure 18. Time-height display of sodar-obtained backscatter on 22 May 94.
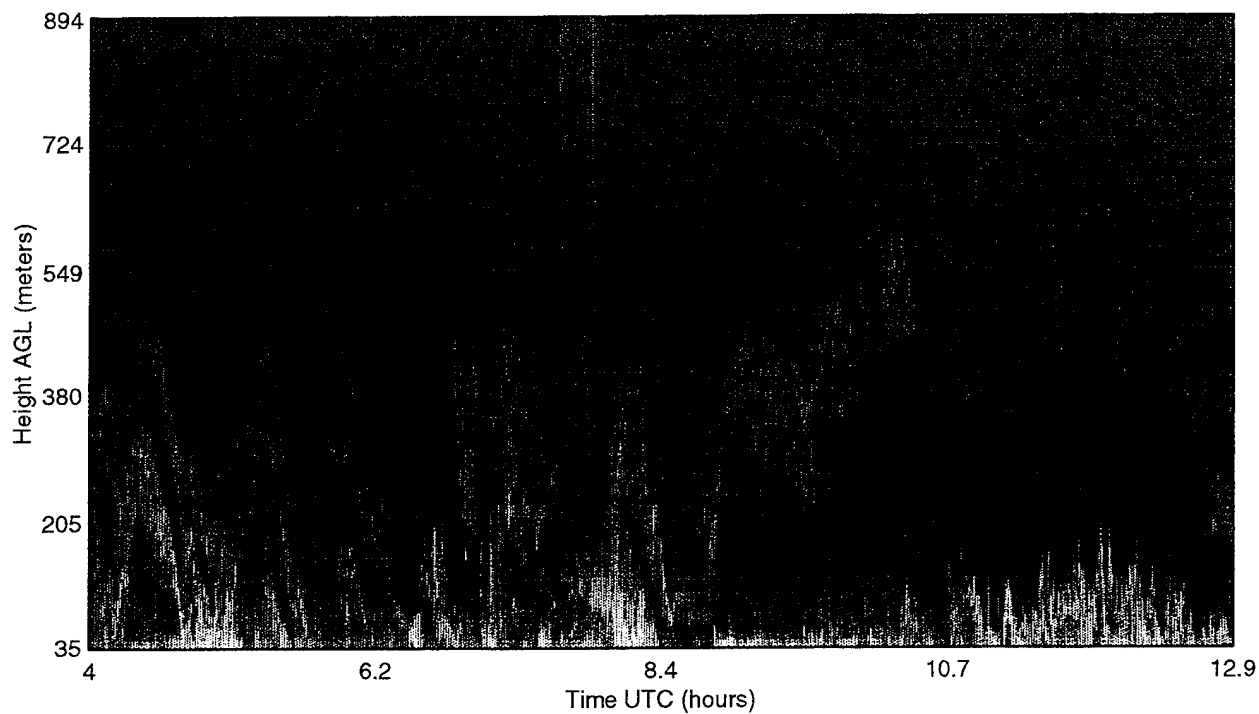
Figure 19. Time-height display of sodar-obtained backscatter on 23 May 94.
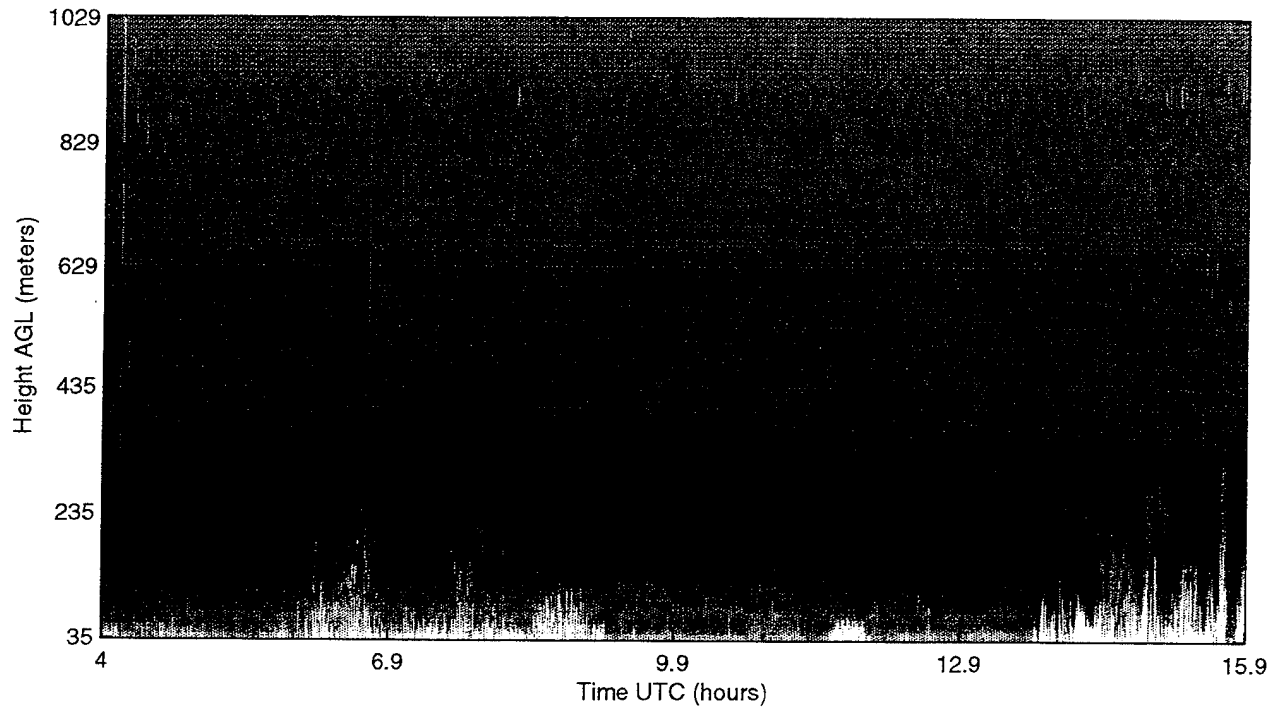
Figure 20. Time-height display of sodar-obtained backscatter on 9 Jun 94.

32
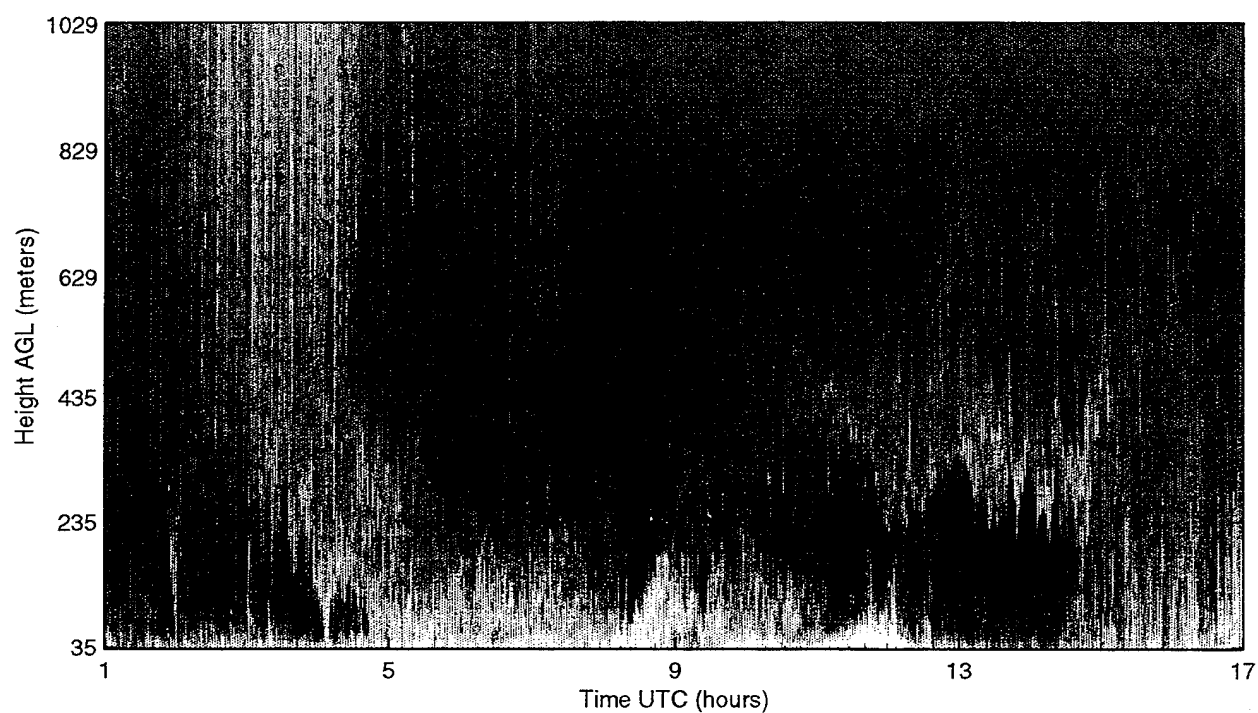
Figure 21. Time-height display of sodar-obtained backscatter on 24 Jun 94 from 0100 to 1700 UTC.
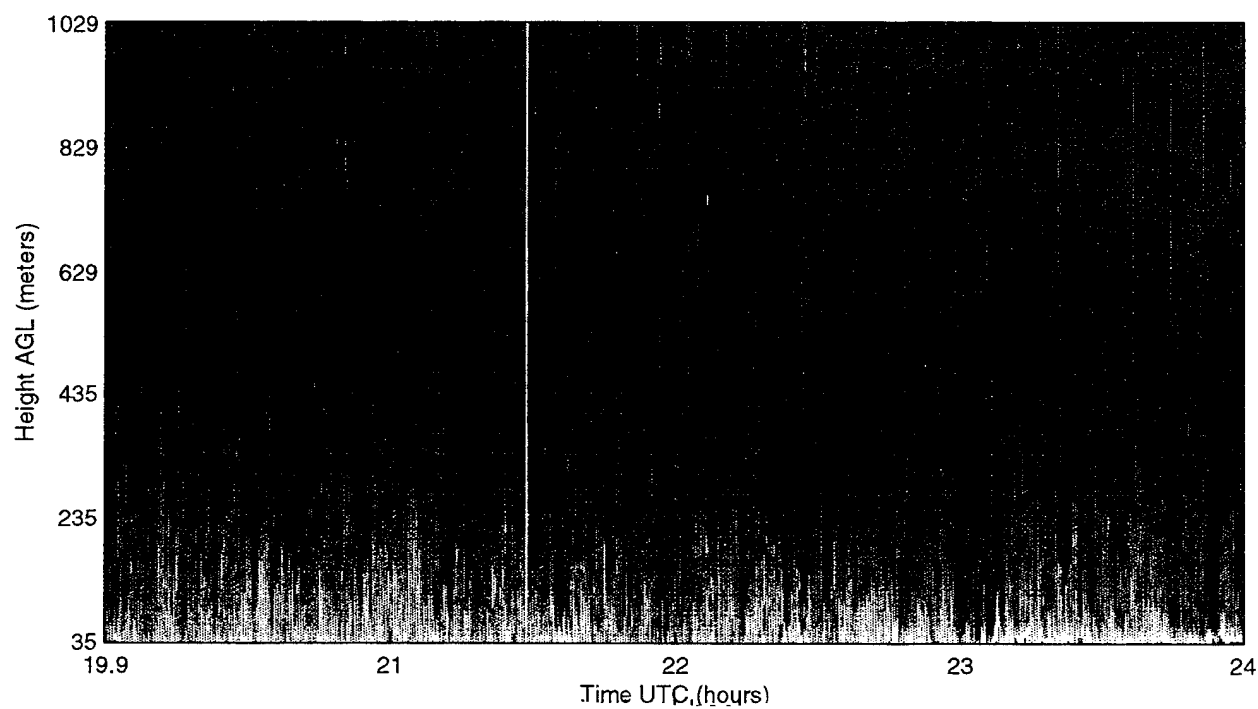
Figure 22. Time-height display of sodar-obtained backscatter on 24 Jun 94 from 1953 to 2400 UTC.

33
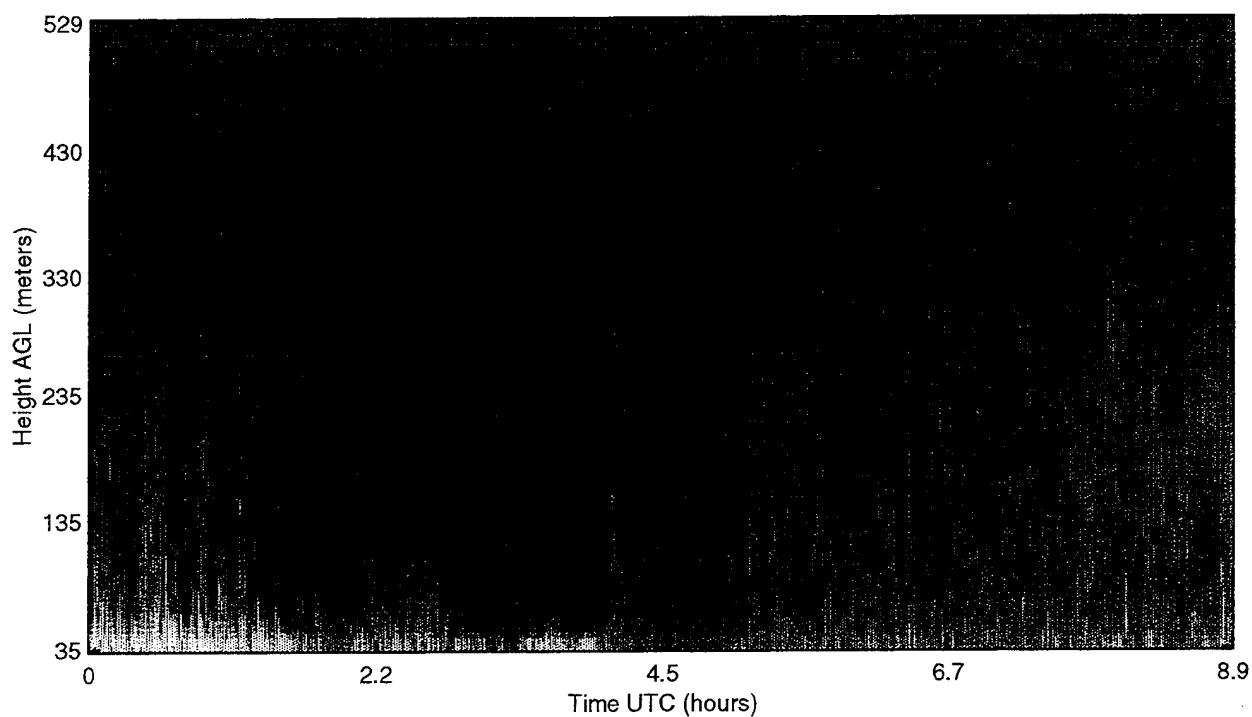
Figure 23. Time-height display of sodar-obtained backscatter on 25 Jun 94.
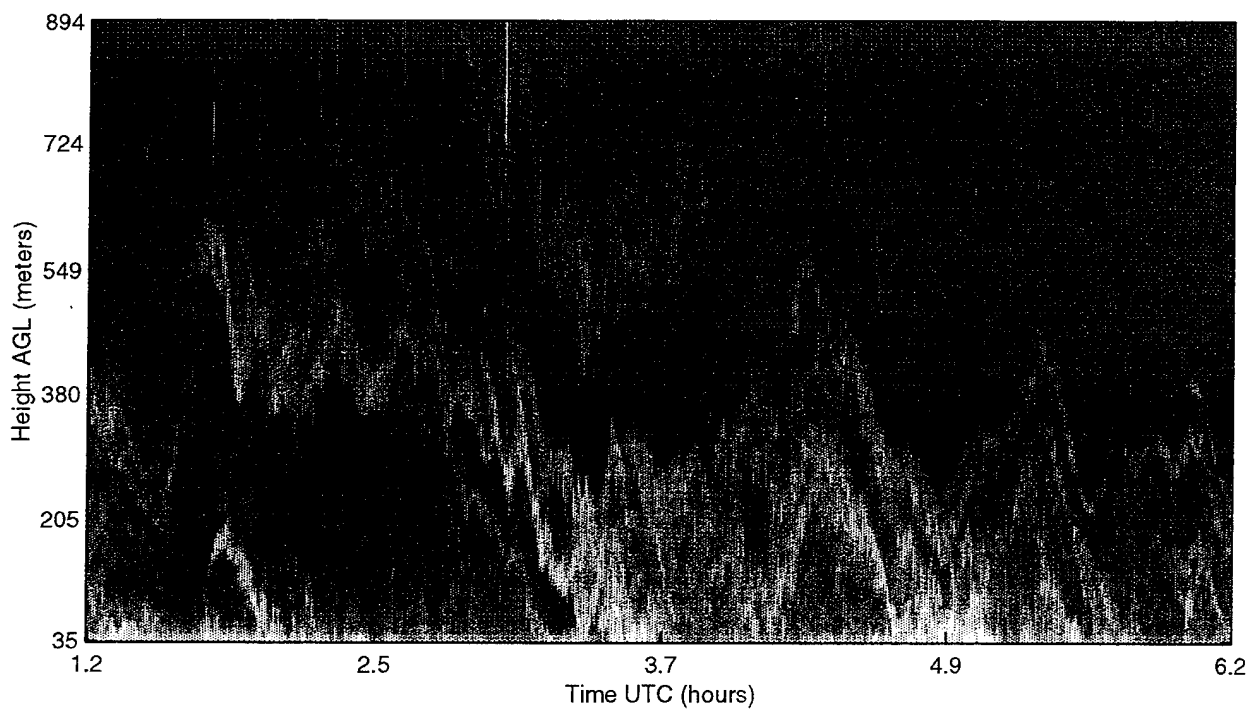
Figure 24. Time-height display of sodar-obtained backscatter showing pronounced wave activity.

34
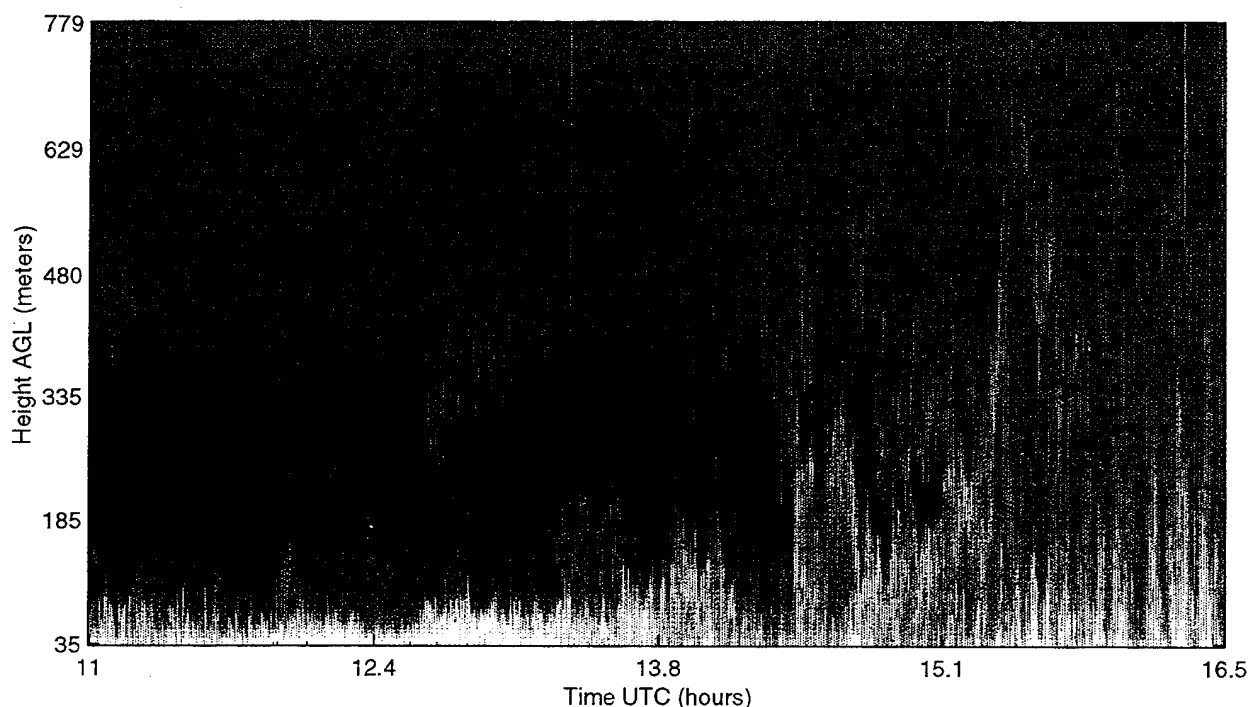
Figure 25. Time-height display of sodar-obtained backscatter showing a morning transition event.

4.4 50-MHz Radar Measurements

Surface wind measurements are often affected by local features. Free air profiles of wind can be measured using doppler radars such as the 50-MHz radar at the APRF. This system also measures profiles of C_n^2. Figures 26 through 32 show 12 h of hourly-averaged wind profiles for each of the 8 days r_o was measured. The first two data periods showed most of the wind to be generally westerly above about 4 km MSL with the highest wind speeds on 23 May between 10 and 15 km MSL. The results during the last data run show mostly northerly flow throughout most of the troposphere. Hourly averages of C_n^2 obtained from 50-MHz radar measurements are shown in figures 33 through 39, corresponding to the wind measurements previously shown. The results show several persistent layers of C_n^2 that are transported with the wind. Figure 40 displays an individual C_n^2 profile, illustrating the layering found in the atmosphere.

35

Figure 26.   Wind speed and direction measured with the 50-MHz radar on 21 May 94.

Figure 27. Wind speed and direction measured with the 50-MHz radar on 22 May 94.

Figure 28. Wind speed and direction measured with the 50-MHz radar on 23 May 94.

Figure 29. Wind speed and direction measured with the 50-MHz radar on 9 Jun 94.

Figure 30. Wind speed and direction measured with the 50-MHz radar on 24 Jun 94 from 0000 to 1100 GMT.

Figure 31. Wind speed and direction measured with the 50-MHz radar on 24 Jun 94 from 1200 to 2300 GMT.

41

Wind Speed and Direction (Wind Barbs)   ALL MODES

ARL 50MHz WSMR, NM   1222 M
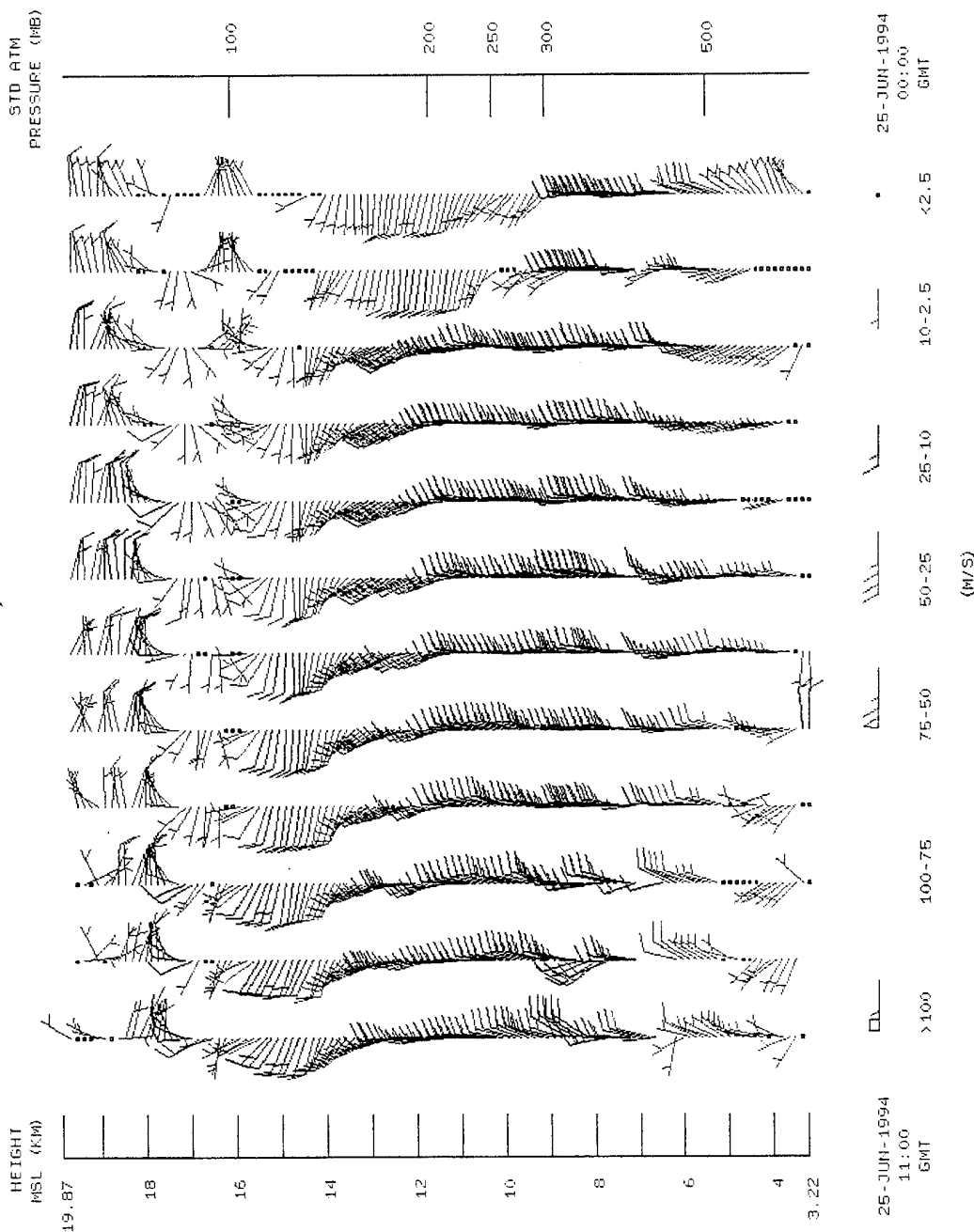
Figure 32. Wind speed and direction measured with the 50-MHz radar on 25 Jun 94.
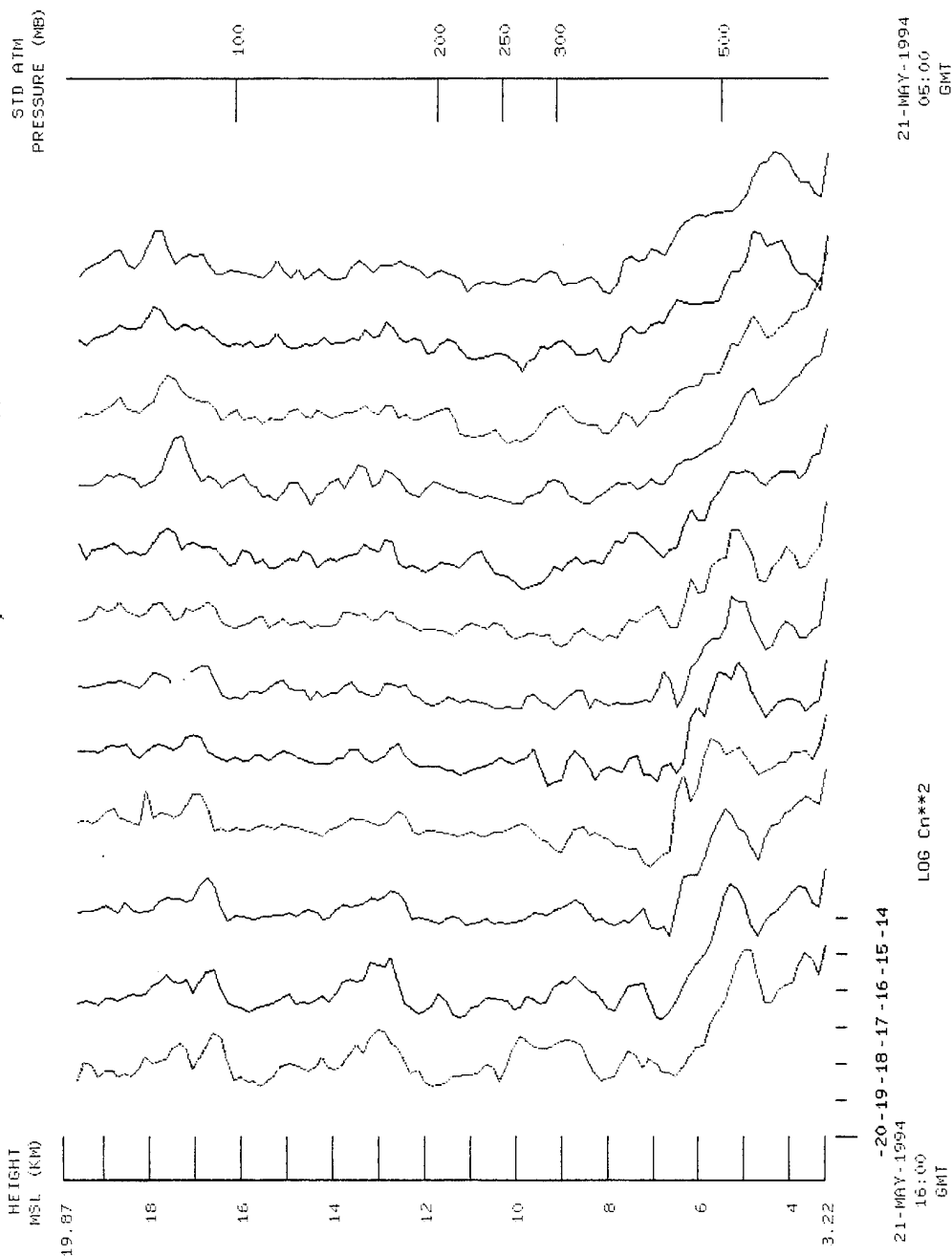
Figure 33. C_n^2 profiles measured with the 50-MHz radar on 21 May 94.

43
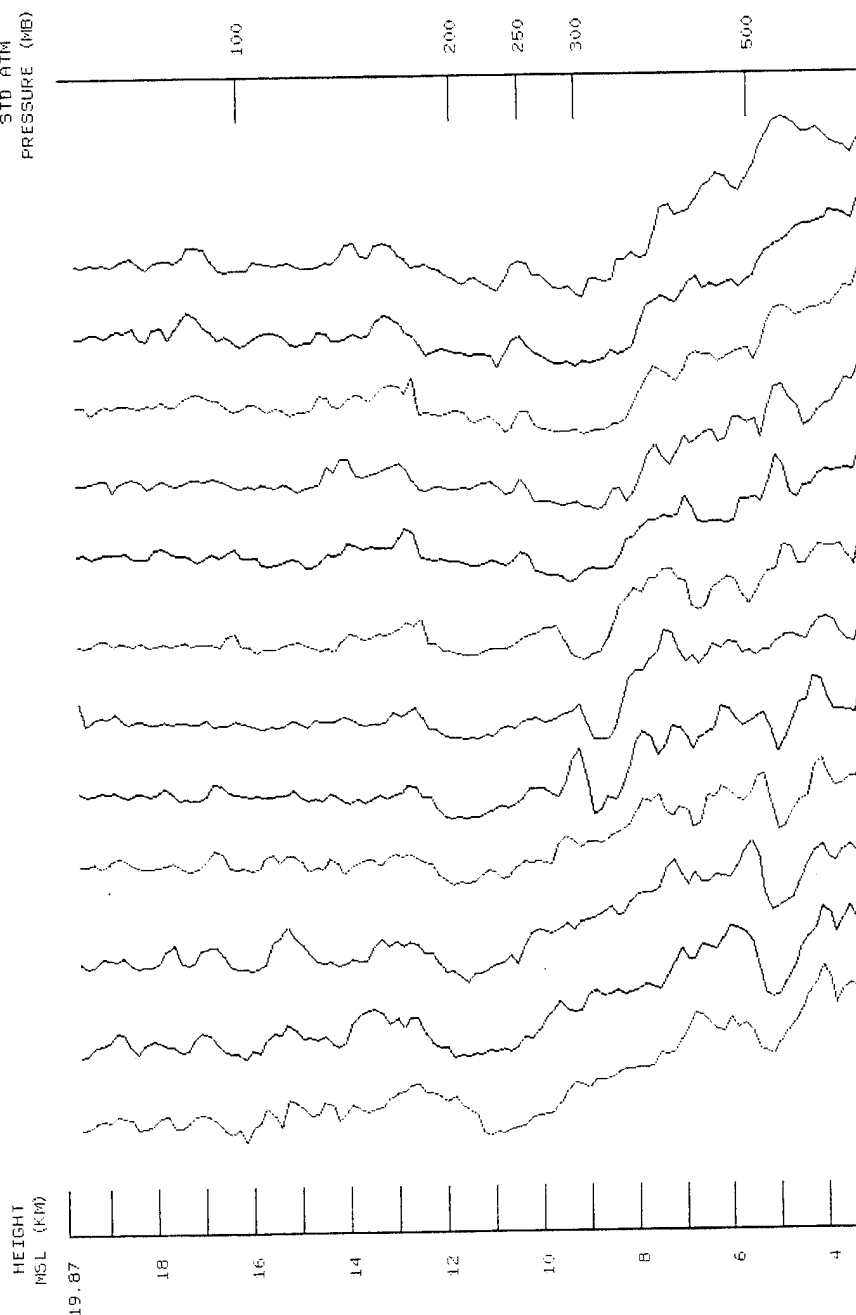
Figure 34. C_n^2 profiles measured with the 50-MHz radar on 22 May 94.
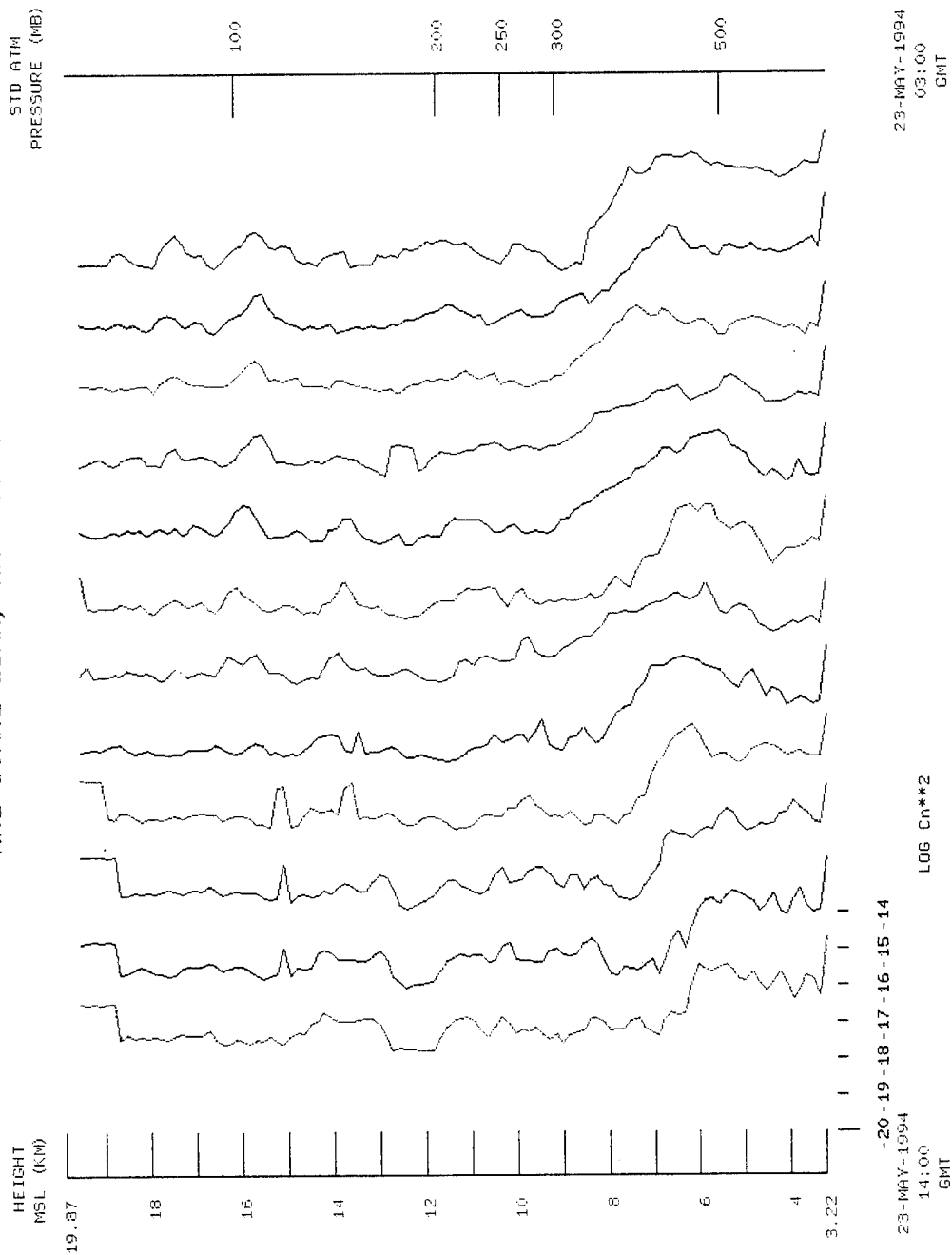
Figure 35. C_n^2 profiles measured with the 50-MHz radar on 23 May 94.
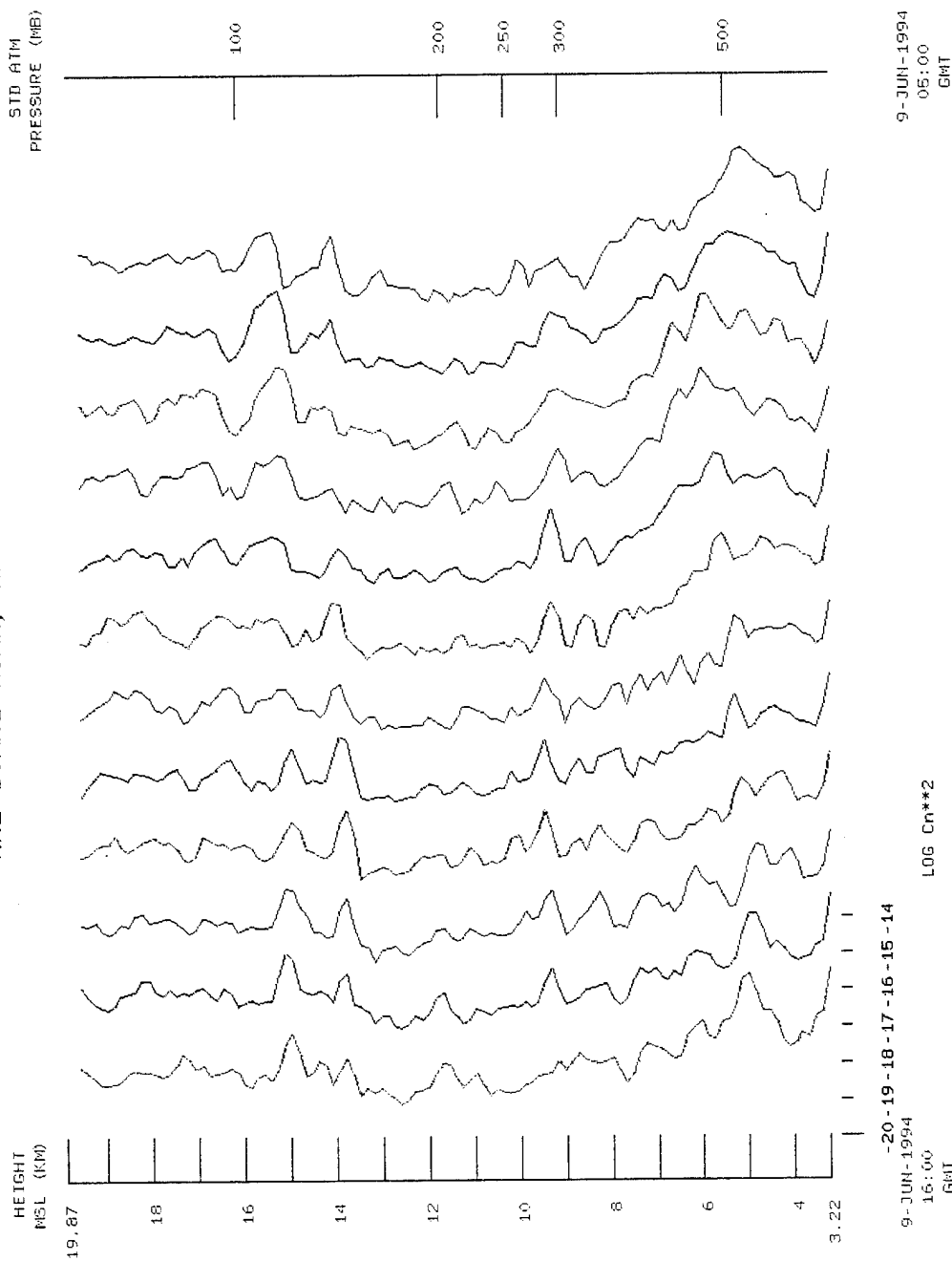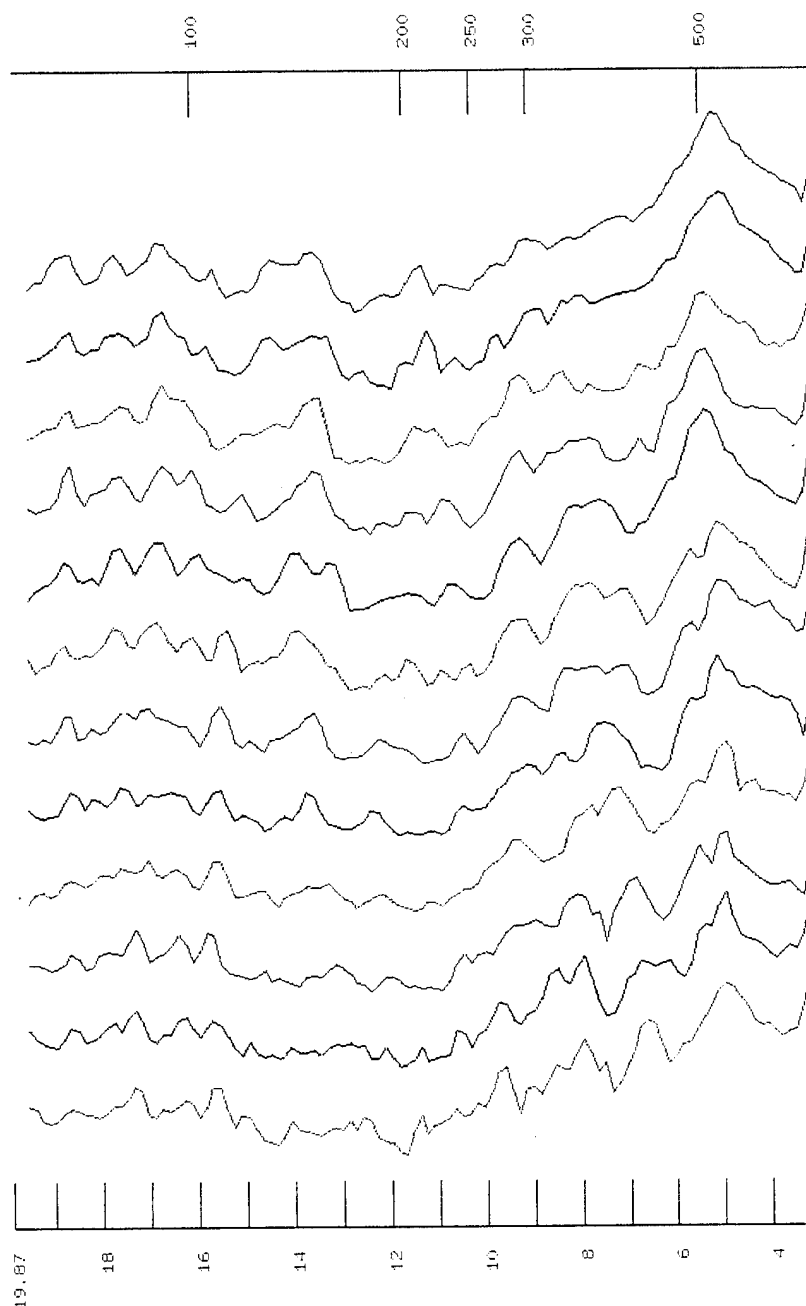
Figure 36. C_n^2 profiles measured with the 50-MHz radar on 9 Jun 94.

Figure 37. C_n^2 profiles measured with the 50-MHz radar on 24 Jun 94 from 0000 to 1100 GMT.

Figure 38. C_n^2 profiles measured with the 50-MHz radar on 24 Jun 94 from 1200 to 2300 GMT.

Figure 39. C_n^2 profiles measured with the 50-MHz radar on 25 Jun 94.
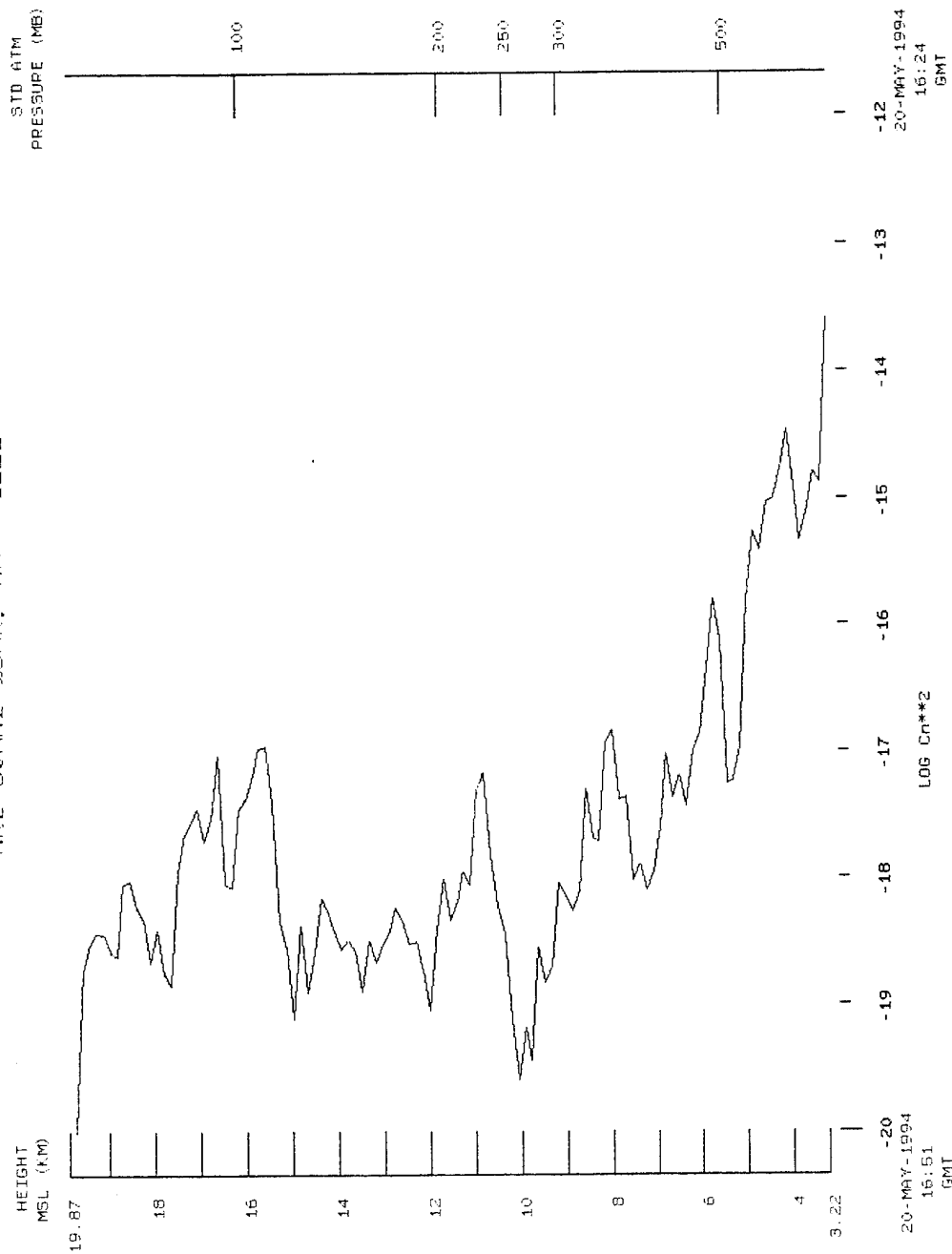
Figure 40. Individual C_n^2 profile expanded to show detail in vertical structure.

5. Summary and Recommendations

Three main points regarding r_0 emerge from the results of this study during spring 94 at APO:

1. Considerable variability in r_0 values, ranging from 1 to 18 cm, was found during nighttime. Data were collected under a variety of wind conditions with the surface wind predominantly coming from forested areas.

2. The onset of the evening neutral event showed a dramatic increase in r_0, presumably caused by radiation balance and associated sensible heat changes on the west-facing slope immediately below ATMOS.

3. Sodar-derived time-height displays of backscattered power (proportional to C_n^2) data obtained at APO show obvious large-scale trends, agreeing with the trends and patterns of r_0. These sodar and r_0 results demonstrate the contribution of local meteorological conditions to r_0.

Recommendations for future research examining r_0 effects at APO include the following:

1. Measure r_0 under different conditions for an extended period to include different wind speed and wind direction conditions, jet stream effects, seasonal effects (with particular emphasis on snow cover), diurnal variation under various atmospheric stabilities, and the evolution of the morning and evening neutral periods.

2. Correlate simultaneous sodar measurements at APO, local meteorological measurements, and 50-MHz radar measurements with the r_0 data to develop a predictive seeing tool. Various parameters calculated from the data such as stability, wind shear, eddy dissipation rate, and gravity wave effects are expected to enhance the predictive capability over correlations of raw data.

References

1. Eaton, F. D., W. A. Peterson, J. R. Hines, K. R. Peterman, R. E. Good, R. R. Beland, and J. H. Brown, "Comparisons of VHF Radar, Optical, and Temperature Fluctuation Measurements of C_n^2, r_o, and θ_o," *Theoretical and Applied Climatology*, 39, pp. 17-29, 1988.

2. Brandt, P. N., H. A. Mauter, and R. Smartt, "Day-Time Seeing Statistics at SPO," *Astronomical Astrophysics*, 188, pp. 163-168, 1987.

3. Fried, D. L., "Optical Resolution Through a Randomly Inhomogeneous Medium for Very Long and Very Short Exposures," *Journal of the Optical Society of America*, 567, pp. 1372-1379, 1966.

4. Babcock, H. W., "Instrumental Recording of Astronomical Seeing," *Publications of the Astronomical Society of the Pacific*, pp. 1-8, 1963.

5. Couder, A., "Optique Atmospherique-Measure Photographique de l'Agitation des Images Stellaries," *Comptes rendus hebdomadaires des s'eances de L'Acad'emie des Sciences, Paris*, 205, pp. 609-611, 1936.

6. Harlan, E. A., and M. F. Walker, "A Star-Trail Telescope for Astronomical Site-Testing," *Publications of the Astronomical Society of the Pacific*, 77, pp. 246-252, 1965.

7. Whitford, A. E., and J. Stebbins, "Photoelectric Measurement of Scintillation of Stars," *Publications of American Astronomy*, 8:228, 1936.

8. Meinel, A. B., "Astronomical Seeing and Observatory Site Selection," *Telescopes*, (ed. G. P. Kuiper and B. M. Middlehurst), Univ. Chicago Press, 1960.

9. Eaton, F. D., W. A. Peterson, J. R. Hines, J. J. Drexler, A. H. Waldie, and D. B. Soules, "Comparison of Two Techniques for Determining Atmospheric Seeing," In *Proceedings SPIE*, Vol. 926, Orlando, FL, pp. 319-334, 1988.

10. Roddier, F., "The Effects of Atmospheric Turbulence in Optical Astronomy," *Progressive Optics*, XIX:283-368, North Holland, 1981.

11. Fried, D. L., "Differential Angle of Arrival: Theory, Evaluation, and Measurement Feasibility," *Radio Science*, 10, pp. 77-86, 1975.

12. Nastrom, G. D., and F. D. Eaton, "The Coupling of Gravity Waves and Turbulence at White Sands, New Mexico, from VHF Radar Observations," *Journal of Applied Meteorology*, Vol. 32, No. 1, pp. 81-87, 1983.

13. Clifford, S. F., "The Classical Theory of Wave Propagation in a Turbulent Medium," *Laser Beam Propagation in the Atmosphere*, edited by J. W. Strohbehm, Springer-Verlag, New York, pp. 11-41, 1978.

14. Kallistratova, M. A., and D. F. Timanovskiy, "The Distribution of the Structure Constant of Refractive Index Fluctuations in the Atmospheric Surface Layer, Izv.," *Atmospheric and Oceanic Physics*, Vol. 7, No. 1, pp. 73-75, 1971.

Acronyms and Abbreviations

APO	Apache Point Observatory
APRF	Atmospheric Profiler Research Facility
ATMOS	Atmospheric Turbulence Measurement and Observation System
CCD	charge-coupled device
SAMS	Surface Atmospheric Measurement System
SDSS	Sloan Digital Sky Survey
SPO	Sacramento Peak Observatory
WSMR	White Sands Missile Range

Distribution

Copies

ARMY CHEMICAL SCHOOL 1
ATZN CM CC
ATTN MR BARNES
FT MCCLELLAN AL 36205-5020

NASA MARSHAL SPACE FLT CTR 1
ATMOSPHERIC SCIENCES DIV
E501
ATTN DR FICHTL
HUNTSVILLE AL 35802

NASA SPACE FLT CTR 1
ATMOSPHERIC SCIENCES DIV
CODE ED 41 1
HUNTSVILLE AL 35812

ARMY STRAT DEFNS CMND 1
CSSD SL L
ATTN DR LILLY
PO BOX 1500
HUNTSVILLE AL 35807-3801

ARMY MISSILE CMND 1
AMSMI RD AC AD
ATTN DR PETERSON
REDSTONE ARSENAL
AL 35898-5242

ARMY MISSILE CMND 1
AMSMI RD AS SS
ATTN MR H F ANDERSON
REDSTONE ARSENAL
AL 35898-5253

ARMY MISSILE CMND 1
AMSMI RD AS SS
ATTN MR B WILLIAMS
REDSTONE ARSENAL
AL 35898-5253

ARMY MISSILE CMND   1
AMSMI RD DE SE
ATTN MR GORDON LILL JR
REDSTONE ARSENAL
AL 35898-5245

ARMY MISSILE CMND   1
REDSTONE SCI INFO CTR
AMSMI RD CS R DOC
REDSTONE ARSENAL
AL 35898-5241

ARMY MISSILE CMND   1
AMSMI
REDSTONE ARSENAL
AL 35898-5253

ARMY INTEL CTR   1
AND FT HUACHUCA
ATSI CDC C
FT HUACHUCA AZ 85613-7000

NORTHROP CORPORATION   1
ELECTR SYST DIV
ATTN MRS T BROHAUGH
2301 W 120TH ST BOX 5032
HAWTHORNE CA 90251-5032

NAVAL WEAPONS CTR   1
CODE 3331
ATTN DR SHLANTA
CHINA LAKE CA 93555

PACIFIC MISSILE TEST CTR   1
GEOPHYSICS DIV
ATTN CODE 3250
POINT MUGU CA 93042-5000

LOCKHEED MIS & SPACE CO   1
ATTN KENNETH R HARDY
ORG 91 01 B 255
3251 HANOVER STREET
PALO ALTO CA 94304-1191

NAVAL OCEAN SYST CTR   1
CODE 54
ATTN DR RICHTER
SAN DIEGO CA 92152-5000

METEOROLOGIST IN CHARGE   1
KWAJALEIN MISSILE RANGE
PO BOX 67
APO SAN FRANCISCO
CA 96555

DEPT OF COMMERCE CTR   1
MOUNTAIN ADMINISTRATION
SPPRT CTR LIBRARY R 51
325 S BROADWAY
BOULDER CO 80303

DR HANS J LIEBE   1
NTIA ITS S 3
325 S BROADWAY
BOULDER CO 80303

NCAR LIBRARY SERIALS   1
NATL CTR FOR ATMOS RSCH
PO BOX 3000
BOULDER CO 80307-3000

DEPT OF COMMERCE CTR   1
325 S BROADWAY
BOULDER CO 80303

DAMI POI   1
WASH DC 20310-1067

MIL ASST FOR ENV SCI OFC   1
OF THE UNDERSEC OF DEFNS
FOR RSCH & ENGR R&AT E LS
PENTAGON ROOM 3D129
WASH DC 20301-3080

DEAN RMD   1
ATTN DR GOMEZ
WASH DC 20314

```
SPACE NAVAL WARFARE                                    1
SYST CMND
PMW 145 1G
WASH DC 20362-5100


ARMY INFANTRY                                          1
ATSH CD CS OR
ATTN DR E DUTOIT
FT BENNING GA 30905-5090


AIR WEATHER SERVICE                                    1
TECH LIBRARY FL4414 3
SCOTT AFB IL 62225-5458


USAFETAC DNE                                           1
ATTN MR GLAUBER
SCOTT AFB IL 62225-5008


HQ AWS DOO 1                                           1
SCOTT AFB IL 62225-5008


ARMY SPACE INSTITUTE                                   1
ATTN ATZI SI 3
FT LEAVENWORTH
KS 66027-5300


PHILLIPS LABORATORY                                    1
PL LYP
ATTN MR CHISHOLM
HANSCOM AFB MA 01731-5000


ATMOSPHERIC SCI DIV                                    1
GEOPHYSICS DIRCTRT
PHILLIPS LABORATORY
HANSCOM AFB MA 01731-5000


PHILLIPS LABORATORY                                    1
PL LYP 3
HANSCOM AFB MA 01731-5000


RAYTHEON COMPANY                                       1
ATTN DR SONNENSCHEIN
528 BOSTON POST ROAD
SUDBURY MA 01776
MAIL STOP 1K9
```

ARMY MATERIEL SYST
ANALYSIS ACTIVITY
AMXSY
ATTN MP H COHEN
APG MD 21005-5071

1

ARMY MATERIEL SYST
ANALYSIS ACTIVITY
AMXSY AT
ATTN MR CAMPBELL
APG MD 21005-5071

1

ARMY MATERIEL SYST
ANALYSIS ACTIVITY
AMXSY CR
ATTN MR MARCHET
APG MD 21005-5071

1

ARL CHEMICAL BIOLOGY
NUC EFFECTS DIV
AMSRL SL CO
APG MD 21010-5423

1

ARMY MATERIEL SYST
ANALYSIS ACTIVITY
AMXSY
APG MD 21005-5071

1

NAVAL RESEARCH LABORATORY
CODE 4110
ATTN MR RUHNKE
WASH DC 20375-5000

1

ARMY MATERIEL SYST
ANALYSIS ACTIVITY
AMXSY CS
ATTN MR BRADLEY
APG MD 21005-5071

1

ARMY RESEARCH LABORATORY
AMSRL D
2800 POWDER MILL ROAD
ADELPHI MD 20783-1145

1

ARMY RESEARCH LABORATORY   1
AMSRL OP SD TP
TECHNICAL PUBLISHING
2800 POWDER MILL ROAD
ADELPHI MD 20783-1145

ARMY RESEARCH LABORATORY   1
AMSRL OP CI SD TL
2800 POWDER MILL ROAD
ADELPHI MD 20783-1145

ARMY RESEARCH LABORATORY   1
AMSRL SS SH
ATTN DR SZTANKAY
2800 POWDER MILL ROAD
ADELPHI MD 20783-1145

ARMY RESEARCH LABORATORY   1
AMSRL
2800 POWDER MILL ROAD
ADELPHI MD 20783-1145

NATIONAL SECURITY AGCY W21   1
ATTN DR LONGBOTHUM
9800 SAVAGE ROAD
FT GEORGE G MEADE
MD 20755-6000

ARMY AVIATION CTR   1
ATZQ D MA
ATTN MR HEATH
FT RUCKER AL 36362

OIC NAVSWC   1
TECH LIBRARY CODE E 232
SILVER SPRINGS
MD 20903-5000

ARMY RSRC OFC   1
ATTN DRXRO GS
PO BOX 12211
RTP NC 27009

DR JERRY DAVIS   1
NCSU
PO BOX 8208
RALEIGH NC 27650-8208

ARMY CCREL   1
CECRL GP
ATTN DR DETSCH
HANOVER NH 03755-1290

ARMY ARDEC   1
SMCAR IMI I BLDG 59
DOVER NJ 07806-5000

ARMY SATELLITE COMM AGCY   1
DRCPM SC 3
FT MONMOUTH NJ 07703-5303

ARMY COMMUNICATIONS   1
ELECTR CTR FOR EW RSTA
AMSEL EW D
FT MONMOUTH NJ 07703-5303

ARMY COMMUNICATIONS   1
ELECTR CTR FOR EW RSTA
AMSEL EW MD
FT MONMOUTH NJ 07703-5303

ARMY DUGWAY PROVING GRD   1
STEDP MT DA L 3
DUGWAY UT 84022-5000

ARMY DUGWAY PROVING GRD   1
STEDP MT M
ATTN MR BOWERS
DUGWAY UT 84022-5000

DEPT OF THE AIR FORCE   1
OL A 2D WEATHER SQUAD MAC
HOLLOMAN AFB
NM 88330-5000

PL WE   1
KIRTLAND AFB NM
87118-6008

USAF ROME LAB TECH   1
CORRIDOR W STE 262 RL SUL
26 ELECTR PKWY BLD 106
GRIFFISS AFB
NY 13441-4514

```
AFMC DOW                                          1
WRIGHT PATTERSON AFB
OH 0334-5000


ARMY FIELD ARTLLRY SCHOOL                          1
ATSF TSM TA
FT SILL OK 73503-5600


NAVAL AIR DEV CTR                                  1
CODE 5012
ATTN AL SALIK
WARMINISTER PA 18974


ARMY FOREGN SCI TECH CTR                           1
CM
220 7TH STREET NE
CHARLOTTESVILLE
VA 22901-5396


NAVAL SURFACE WEAPONS CTR                          1
CODE G63
DAHLGREN VA 22448-5000


ARMY OEC                                           1
CSTE EFS
PARK CENTER IV
4501 FORD AVE
ALEXANDRIA VA 22302-1458


ARMY CORPS OF ENGRS                                1
ENGR TOPOGRAPHICS LAB
ETL GS LB
FT BELVOIR VA 22060


TAC DOWP                                           1
LANGLEY AFB
VA 23665-5524


ARMY TOPO ENGR CTR                                 1
CETEC ZC 1
FT BELVOIR VA 22060-5546


LOGISTICS CTR                                      1
ATCL CE
FT LEE VA 23801-6000
```

64

SCI AND TECHNOLOGY   1
101 RESEARCH DRIVE
HAMPTON VA 23666-1340

ARMY NUCLEAR CML AGCY   1
MONA ZB BLDG 2073
SPRINGFIELD VA 22150-3198

ARMY FIELD ARTLLRY SCHOOL   1
ATSF F FD
FT SILL OK 73503-5600

USATRADOC   1
ATCD FA
FT MONROE VA 23651-5170

ARMY TRADOC ANALYSIS CTR   1
ATRC WSS R
WSMR NM 88002-5502

ARMY RESEARCH LABORATORY   1
AMSRL BE M
BATTLEFIELD ENVIR DIR
WSMR NM 88002-5501

ARMY RESEARCH LABORATORY   1
AMSRL BE A
BATTLEFIELD ENVIR DIR
WSMR NM 88002-5501

ARMY RESEARCH LABORATORY   1
AMSRL BE W
BATTLEFIELD ENVIR DIR
WSMR NM 88002-5501

ARMY RESEARCH LABORATORY   1
AMSRL BE
ATTN MR VEAZEY
BATTLEFIELD ENVIR DIR
WSMR NM 88002-5501

DEFNS TECH INFO CTR   1
CENTER DTIC BLS
BLDG 5 CAMERON STATION
ALEXANDRIA
VA 22304-6145

ARMY MISSILE CMND   1
AMSMI
REDSTONE ARSENAL
AL 35898-5243

ARMY DUGWAY PROVING GRD   1
STEDP 3
DUGWAY UT 84022-5000

USATRADOC   1
ATCD FA
FT MONROE VA 23651-5170

ARMY FIELD ARTLRY SCHOOL   1
ATSF
FT SILL OK 73503-5600

WSMR TECH LIBRARY BR   1
STEWS IM IT
WSMR NM 88001

Record Copy   10

TOTAL   96